HISTORY-MATCHING PRODUCTION DATA USING ENSEMBLE SMOOTHER WITH MULTIPLE DATA ASSIMILATION: A COMPARATIVE STUDY

A Thesis

by

Xiaoyang Xia

Submitted to the Office of Graduate and Professional Studies of
Texas A&M University
in partial fulfillment of the requirements for the degree of

MASTER OF SCIENCE

Chair of Committee,	Akhil Datta-Gupta
Committee Members,	Michael King
	Bani K. Mallick
Head of Department,	A. Daniel Hill

Dec 2014

Major Subject: Petroleum Engineering

Copyright 2014 Copyright Xiaoyang Xia

ABSTRACT

Reservoir simulation models are generated by petroleum engineers to optimize field operation and production, thus maximizing oil recovery. History matching methods are extensively used for reservoir model calibration and petrophysical properties estimation by matching numerical simulation results with true oil production history. Sequential reservoir model updating technique Ensemble Kalman filter (EnKF) has gained popularity in automatic history matching because of simple conceptual formulation and ease of implementation. The computational cost is relatively affordable compared with other sophisticated assimilation methods. Ensemble Smoother is a viable alternative of EnKF. Unlike EnKF, Ensemble Smoother computes a global update by simultaneously assimilating all data available and provides a significant reduction in simulation time. However, Ensemble Smoother typically yields a data match significantly inferior to that obtained with EnKF. Ensemble smoother with multiple data assimilation (ES-MDA) is developed as efficient iterative forms of Ensemble Smoother to compare with conventional EnKF.

For ES-MDA the same set of data is assimilated multiple times with an inflated covariance matrix of the measurement error. We apply ES-MDA and EnKF to generate multiple realizations of the permeability field by history matching production data including bottom-hole pressure, water-cut and gas-oil ratio. Both algorithms have been implemented to synthetic heterogeneous case and Goldsmith field case. Moreover, ES-MDA coupled

with various covariance localization methods: Distance based, Streamline based and Hierarchical ensemble filter localization methods are compared in terms of both quality of history matching and permeability distribution.

DEDICATION

To my beloved father, mother and brother for supporting and loving me. To my beloved

wife Yi Zhang, for her consistent encouragement, respect and affection to me.

ACKNOWLEDGEMENTS

NOMENCLATURE

C	Connectivity matrix
$\mathbf{C_D}$	Data covariance matrix
$C_{M^s,d}$	Cross-covariance matrix between data and model parameters
$\mathbf{C}_K^P$	Updated model covariance matrix
D	Diagonal matrix of eigenvalues of the matrix F
$D_{obs,k}$	Ensemble of the observation data
d_{obs}	Observation data vector
d_k^{cal}	Calculated or theoretical observation vector
d_{true}	True observation data vector
E	Connectivity matrix with the mean vector subtracted
F	Covariance matrix of matrix E
ε_k	Measurement error
H	Measurement matrix
K	Absolute Permeability
K_k	Kalman Gain
$log(K)$	Log of absolute permeability
k_r	Relative permeability
m_k^{sta}	Vector of static model variables
m_k^{dyn}	Vector of dynamic model variables
N_d	Number of observation data
N_e	Number of ensemble members
ρ	Covariance localizing function
R^N	N numbers of real numbers

t	Time
y_k	Model state vector
y_{N_{states}, N_e}	Augmented Model state vector
x_i	Vector incorporated into calculating Euclidean distance
$\delta_{i,j}$	Euclidean distance
V	Matrix of eigenvectors

TABLE OF CONTENTS

LIST OF FIGURES

LIST OF TABLES

CHAPTER I

INTRODUCTION

Reservoir simulation models are generated by petroleum engineers to optimize field operation and production, thus maximizing oil recovery. History matching methods are extensively used for reservoir model calibration and petrophysical properties estimation by matching numerical simulation results with oil production history.

Background of Ensemble Kalman Filter (EnKF) and Ensemble Smoother with Multiple Data Assimilation (ES-MDA)

Sequential reservoir model updating technique Ensemble Kalman filter (EnKF) has gained popularity in automatic history matching because of simple conceptual formulation and ease of implementation. The computational cost is relatively affordable compared with other sophisticated assimilation method. Ensemble Smoother is a viable alternative of EnKF. Unlike EnKF, Ensemble Smoother computes a global update by simultaneously assimilating all data available and provides a significant reduction in simulation time. However, Ensemble Smoother typically yields a data match significantly inferior to that obtained with EnKF. Ensemble smoother with multiple data assimilation (ES-MDA) is developed as efficient iterative forms of Ensemble Smoother to compare with conventional EnKF.

For ES-MDA the same set of data is assimilated multiple times with an inflated covariance matrix of the measurement error. We apply ES-MDA and EnKF to generate multiple realizations of the permeability field by history matching production data including bottom-hole pressure, water-cut and gas-oil ratio. Both algorithms have been implemented to synthetic heterogeneous case and Goldsmith field case. Moreover, ES-MDA coupled with various covariance localization methods: Distance based, Streamline based and Hierarchical ensemble filter localizations are compared in terms of both quality of history matching and permeability distribution.

Ensemble Kalman Filter (EnKF) is a data assimilation technique that has gained increasing interest in the application of petroleum history matching in recent years. The basic methodology of the EnKF consists of the forecast step and the update step. This data assimilation method utilizes a collection of state vectors, known as an ensemble, which are simulated forward in time. In other words, each ensemble member represents a reservoir model (realization). Subsequently, during the update step, the sample covariance is computed from the ensemble, while the collection of state vectors is updated using the formulations which involve this updated sample covariance.

Objectives of Covariance Localization Study

Covariance localization basically means localizing the effect of an observation to the state variables that are 'closer' to the observations. The various localization methods proposed in the literature have the common goal of removing the spurious terms in the cross-

covariance matrix, this matrix is in turn used to update the state vectors during the EnKF update process. This is done by conditioning the Kalman Gain through a localizing function. Each localization scheme distinguishes itself from each other by how this localizing function, also known as the Schur product or the multiplier function, is computed.

The motivation of covariance localization is to achieve a similar level of EnKF performance if a larger ensemble size would have been used. However, it requires enormous computational resources to perform history matching if the ensemble size is large. Various cases of EnKF with and without localization are implemented on a highly heterogeneous synthetic field case. In this thesis, we will describe the methodology of each localization scheme with their characteristics and limitations on this kind of case setting. To judge the effectiveness of each covariance localization method, the quality of the dynamic response history match and the performance of parameter estimation with respect to the reference model are the main parameters examined.

Literature Review

In the past twenty years ensemble based methods have been widely investigated and implemented in sequential data assimilation and automatic reservoir history matching for reservoir characterization problem. The Ensemble Kalman Filter (EnKF) (Evensen 1994) which can combine uncertainty in the reservoir description and the reservoir performance predictions is the most popular history matching method. Some significant developments

of EnKF have been made to estimate poorly known parameters and to improve the predictive capacity of reservoir models.

Traditional Kalman filter was first introduced in 1960s for cases which have a small number of parameters and the relationship between model parameters and data observation is linear. Extended Kalman filter was introduced afterwards trying to solve nonlinear problems. Due to the high nonlinearity of reservoir engineering problem, traditional Kalman filter is not appropriate for automatic history matching problem. In 1994 Evensen proposed a new methodology that utilizes Kalman filters for large nonlinear models (Evensen 1994). This technique is known as the Ensemble Kalman filter (EnKF). In EnKF framework, an ensemble of reservoir model realizations is continuously updated as the new observation data becomes available. The sequential data assimilation step includes a forecast step and a update step. The forecast is to propagate the ensemble forward in time and the update step is to modify the reservoir parameters in order to match the current observations. EnKF can be linked to any existing reservoir simulator and is able to assimilate the latest production data without re-running the simulator from the initial conditions. All these features make EnKF feasible for continuous reservoir model updating and a viable approach to characterize reservoir compared with other traditional history matching techniques. Due to such advantages of EnKF, great interest in EnKF and its application in automatic history matching has been generated.

Since 2003, the EnKF has been applied in diverse research fields including weather prediction (I. Szunyogh 2005), oceanography (C.L. Keppenne 2003), hydrology (Y. Chen 2006) and petroleum field-scale reservoir characterization problems (Nævdal 2002, Emerick 2011). Two recent review papers (Aanonsen 2009, Oliver 2010) summarize the main developments and applications of EnKF in reservoir history-matching problems. Despite the increasing amount of publications addressing EnKF for history matching and parameter estimation, there are still some problems associated with EnKF application. One disadvantage of the EnKF is the Gaussian approximation applied in the update schemes. Liu and Oliver (Liu 2005) recognized that the Gaussian approximation may be too severe in strongly non-Gaussian problem and this would lead to inconsistent, unphysical solutions and generate numerical instabilities. Another problem is the repeated simulation restarts required by the sequential data assimilation are inconvenient and there is a chance of restarting from inconsistent and unphysical model states. Other EnKF problems are ensemble collapse and filter divergence.

The Ensemble Smoother (ES), an alternative data assimilation method was introduced by van Leeuwen and Evensen (P.J. van Leeuwen 1996). Different from EnKF, ES does not assimilate data sequentially in time and ES computes a global update in one go by simultaneously assimilating all data available without recursively updating in time. Van Leeuwen and Evensen (P.J. van Leeuwen 1996) recognized that ES typically yields a data match significantly inferior to that obtained with EnKF in an ocean circulation model. Evensen and van Leeuwen (G. Evensen 2000) compared ES and EnKF with

Lorenz equations and concluded that EnKF outperforms ES due to the recursive updates in EnKF keep the ensemble of states "on track" and closer to the true solution. Skjervheim et al.(Skjervheim 2011) compared performance of ES and EnKF and concluded that both methods show similar results and acceptable history matches are obtained for the reservoir history-matching problem in both synthetic case and a real North-Sea field application. The major advantage of ES is that it avoids updating the reservoir model recursively and restarts for each ensemble member. Skjervheim et al. showed that ES only required 10% computational cost of EnKF in the real North-Sea field application.

Emerick and Reynolds (A.C. Reynolds 2006, Alexandre A. Emerick 2012) introduced a method based on assimilating the same data set multiple times with covariance matrix of measurement errors multiplied by number of data assimilations. Emerick and Reynolds (2012) proved that single and multiple data assimilation (MDA) are equivalent for the linear-Gaussian case and computational evidence is shown for that MDA can improve EnKF parameter estimation performance for the nonlinear case. Emerick and Reynolds (2012) applied idea of multiple data assimilation to two phase synthetic reservoir model and Brugge field case for production data history match. Both cases show that Ensemble Smoother performed poorly compared with EnKF and ES-MDA. ES-MDA can generate better production data match than EnKF with less expensive computational cost.

Emerick and Reynolds (Alexandre A. Emerick 2013) presented a field application of EnKF and ES-MDA for production data and 3D and 4D seismic data history matching.

ES-MDA achieved better history matching compared with EnKF with only 4% higher computational costs. Emerick and Reynolds (2013) also tested different number of data assimilation for history matching performance and computational cost.

Thesis Outline

In this chapter, we give a general description of the Ensemble Kalman Filter (EnKF) and Ensemble Smoother with Multiple Data Assimilation (ES-MDA). We discuss the motivation for Ensemble Smoother with Multiple Data Assimilation application.

In Chapter II, we discuss the mathematical formulations of the EnKF and ES-MDA in details, the advantages and limitation for both algorithms.

In Chapter III, we discuss the performance of EnKF and ES-MDA in the application of synthetic reservoir models and Goldsmith field case. Water-cut, gas oil ratio (GOR) and bottom-hole pressure history matching performance are compared. Updated permeability field and permeability variance are cross-checked with true case.

In Chapter IV, we test different number of data assimilation and inflation coefficients for history matching performance and computational cost for ES-MDA.

In Chapter V, we apply different ES-MDA covariance localization methods to synthetic reservoir models and Goldsmith field case. We also compare the history matching quality of the different covariance localization schemes.

In Chapter VI, we conclude and make recommendations for future work.

CHAPTER II

MATHMATICAL FORMULATIONS FOR ENSEMBLE KALMAN FILTER AND ENSENMBLE SMOOTHER WITH MULTIPLE DATA ASSIMILATION

In this chapter, the Ensemble Kalman Filter and Ensemble Smoother formulation are generalized for the scope of reservoir characterization and history matching. Furthermore, recent progress and formulation of Ensemble Smoother with Multiple Data Assimilation are introduced. The mathematical assumptions and limitations for above formulations are also discussed.

Mathematical Formulations for Ensemble Kalman Filter

The traditional EnKF is composed of two mains steps: the forecast step and update step. As is shown in Figure 1 for case of water cut history matching case, the forecast step is to predict and propagate state vectors including water cut from time step 1 to time step 2. During this step the state vectors of all ensemble members are advanced. The number of ensemble members can vary from a few to thousands and the ensemble members stand for a range of reservoir models to simulate real reservoir. During this data assimilation, the state vectors are propagated by using a reservoir simulator Eclipse (commercial reservoir simulator developed by Schlumberger).
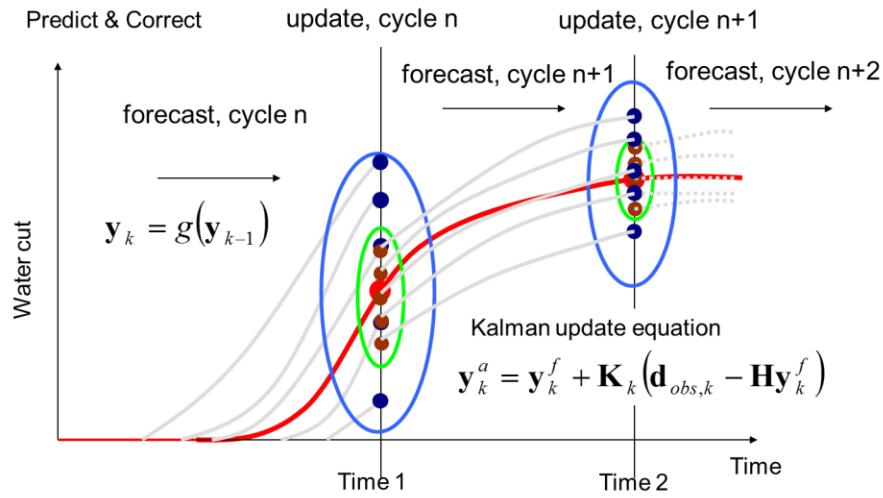
Figure 1: Flow diagram for Ensemble Kalman Filter predict and update process

Subsequently, for second update step, the various water cut data generated by the ensemble members are compared with true water cut production data. The discrepancy between the simulation water cut results and true production data are analyzed and corrected by Kalman Update Equation. Correspondingly , the blue point in Figure 1 in time 1 are initial ensemble results propagated from time 0 and updated ensemble results are shown red dots. The state vectors are also updated at the same time. The forecast and update steps are repeated for following data assimilation time until the most recent history. Through repeated forecast and update steps EnKF is able to sequentially assimilate production data and update reservoir model. The quality of production data history matching is also improved during step by step data assimilation.

Model Parameters m_k^{sta} are parameters that varies with time. They are also called static model variables, which include reservoir parameters such as permeability and porosity. State variables m_k^{dyn} are also called dynamic model variables, which normally include pressure and phase saturations. These parameters are solved by governing partial differential equations (Eclipse). Observation data are true production data which include well measurement data and spatial data. In this thesis, water cut (WWCT), gas oil ratio (GOR) and bottom-hole pressure (WBHP) are history matched.

State Vector y_k is an augmented vector which consists of above parameters: model static and dynamic variables, calculated observation data.

$$y_k = \begin{Bmatrix} m_k^{\mathbf{sta}} \\ m_k^{dyn} \\ d_k^{cal} \end{Bmatrix} \quad \dots\dots\dots\dots\dots\dots\dots\dots\dots\dots\dots\dots\dots\dots \text{(2.1)}$$

This state vector is consistently updated in EnKF. For the ensemble of models, we collect each model state vector and form an ensemble of state vectors. EnKF essentially update this matrix through step by step data assimilation.

In nine spot heterogeneous case and Goldsmith field case, the state vector include log permeability, pressure, water-cut, saturation and bottom-hole pressure. The ensemble Kalman filter (EnKF) utilizes an ensemble of state vectors other than a single state vector.

11

The statistics (mean and covariance) are then computed from the ensemble; the ensemble of state vectors can be represented by the equation 2.2.

$$\Psi_k^p = \left\{ y_{k,1}^p \quad y_{k,2}^p \quad \cdots \quad y_{k,N_e}^p \right\}$$ …………………………………………….. (2.2)

Where the superscript p denotes prior, k denotes time and Ne denotes ensemble number. Each state vector stands for model which is an infinite ensemble of states that are consistent with initial measurement from well logs, core and seismic. Initial ensemble can be generated by geostatistics techniques like sequential Gaussian simulation, for example using SGEMS, a public domain software.

The calculated observation data is related by measurement matrix H with state vector at time k:

$$d_{cal,k} = Hy_k$$ …………………………………………………………………… (2.3)

Measurement matrix H is given by equation 2.4 where I is the identity matrix.

$$H = \begin{bmatrix} 0 & I \end{bmatrix}$$ …………………..………………………………………...…..…… (2.4)

Forecast Step and Update Step

After initial ensemble is generated by SGEMS, forecast step is achieved by calling forward reservoir simulator Eclipse. Forward model is to relate calculated observation data with model static and dynamic variables. This is carried out by solving governing differential equation and discretization in time and space. The calculated observation data is derived from model static and dynamic variables. We can also relate true observed data to model static and dynamic variables with measurement noise.

$$\begin{Bmatrix} m_k^d \\ d_{cal,k} \end{Bmatrix} = g(m_{k-1}^s, m_{k-1}^d) \ \dots\dots\dots\dots\dots\dots\dots\dots\dots\dots\dots\dots\dots \ (2.5)$$

In update step, updated ensemble of state vectors are closely related with data discrepancy between true observation data and calculated data as mentioned in equation 2.4 and 2.5.

$$\psi_k^u = \psi_k^p + K\left(D_k - H\psi_k^p\right) \ \dots\dots\dots\dots\dots\dots\dots\dots\dots\dots\dots\dots \ (2.6)$$

The superscript u denotes updated ensemble of state vectors and p denotes prior ensemble of state vectors. Matrix D is an ensemble of perturbed observations data and matrix K is the Kalman gain matrix. Measurement matrix H is to choose corresponding rows in ψ_k^p to compare with related calculated observation data $d_{cal,k}$

The Kalman gain matrix is shown below:

$$K = C_{\Psi,k}^p H^T \left(H C_{\Psi,k}^p H^T + C_D\right)^{-1} \ \dots\dots\dots\dots\dots\dots\dots\dots\dots\dots\dots \ (2.7)$$

Where $C_{\Psi,k}^p$ represent an estimate of the state vector covariance matrix C_y and C_D represent observation covariance matrix. Matrix D, the ensemble of perturbed observations is shown below:

$$D_k = \{d_{k,1} \quad d_{k,2} \quad \dots \quad d_{k,N_e}\} \ \dots\dots\dots\dots\dots\dots\dots\dots\dots\dots \ (2.8)$$

$$d_{k,i} = d_k + \varepsilon_i \ \dots\dots\dots\dots\dots\dots\dots\dots\dots\dots\dots\dots\dots\dots \ (2.9)$$

Where $d_{k,i}$ is production data vector at time k for ensemble number i. Production data can be water-cut, bottom-hole pressure, gas oil ratio or seismic data; ε_i represents data noise for ensemble number i. The noise is assumed to be normally distributed with mean zero a covariance given by C_D.

The observed data $d_{k,i}$ typically has measurement error subject to physical data uncertainty. The true production data is assumed to have no noise, so the observable data is the perturbed observation vector from true production data. It is obtained by adding random noise ε_k to the "true" observation d_{true} (Burgers, Leeuwen et al. 1998). Error ε_i represents the measurement error at time k. The actual value of ε_i is unknown and it is assumed to be a Gaussian distribution with zero mean value.

Observation error covariance matrix is defined as

$$C_{D,k} = E[\varepsilon_k \varepsilon_k^T] = \overline{\varepsilon_k \varepsilon_k}^T \qquad\qquad (2.10)$$

For this case, the errors in the observation data are not correlated, therefore $C_{D,k}$ turns out to be a diagonal matrix.

Back to Kalman gain equation, $C_{\Psi,k}^P$ represent an estimate of the state vector covariance matrix at time k. $C_{\Psi,k}^P$ is defined as:

$$C_k^P = \frac{1}{N_e - 1} \sum_{j=1}^{N_e} (y_{k,i}^P - y_{k,true}^P)(y_{k,i}^P - y_{k,true}^P)^T \qquad\qquad (2.11)$$

Since the actual state vector is unknown, it is approximated by the mean of the ensemble state vectors.

$$C_k^P = \frac{1}{N_e - 1} \sum_{j=1}^{N_e} (y_{k,i}^P - \bar{y}_k^P)(y_{k,j}^P - \bar{y}_k^P)^T \qquad\qquad (2.12)$$

Where $\overline{y}_k^p$ is the mean value of all ensemble state vectors:

$$\overline{y}_k^p = \frac{1}{N_e} \sum_{i=1}^{N_e} y_{k,i}^P \quad \dots\dots\dots\dots\dots\dots\dots\dots\dots\dots\dots\dots\dots\dots\dots\dots\dots\dots\dots \quad (2.13)$$

The covariance matrix of the state vector is represented as:

$$C^P = \begin{pmatrix} C_{\mathbf{m}^{sta}} & C_{\mathbf{m}^{sta},\mathbf{m}^{dym}} & C_{\mathbf{m}^{sta},\mathbf{d}^{cal}} \\ C_{\mathbf{m}^{dym},\mathbf{d}^{cal}}^{\mathbf{T}} & C_{\mathbf{m}^{dym}} & C_{\mathbf{m}^{dym},\mathbf{d}^{cal}} \\ C_{\mathbf{m}^{sta},\mathbf{d}^{cal}}^{\mathbf{T}} & C_{\mathbf{m}^{dym},\mathbf{d}^{cal}}^{\mathbf{T}} & C_{\mathbf{d}^{cal}} \end{pmatrix}^p \quad \dots\dots\dots\dots\dots\dots\dots \quad (2.14)$$

The covariance matrix of the static variables $C_{m^{sta}}$ and the dynamic variables $C_{m^{dyn}}$ both

have a matrix size of $N_m \times N_m$ where N_m is the number of grid blocks. The covariance

matrix of the calculated data $C_{d^{cal}}$ has a matrix size of $N_d \times N_d$ where N_d is the

number of measurement data at time k. Non-diagonal elements like $C_{m^{sta},m^{dym}}$ and $C_{m^{sta},d^{cal}}$

are cross covariance matrix of calculated data and the state variables. Since C^P is defined

in the above equation, we can easily define the cross covariance matrices $C^P H^T$ and also

$HC^P H^T$.

$$C^P H^T = \begin{pmatrix} C_{m^{sta}} & C_{m^{sta},m^{dym}} & C_{m^{sta},d^{cal}} \\ C_{m^{dym},d^{cal}}^{T} & C_{m^{dym}} & C_{m^{dym},d^{cal}} \\ C_{m^{sta},d^{cal}}^{T} & C_{m^{dym},d^{cal}}^{T} & C_{d^{cal}} \end{pmatrix}^p \begin{pmatrix} 0 \\ 0 \\ 1 \end{pmatrix} = \begin{pmatrix} C_{m^{sta},d^{cal}} \\ C_{m^{dym},d^{cal}} \\ C_{d^{cal}} \end{pmatrix}^P \quad \dots (2.15)$$

And

$$HC^P H^T = C_{d^{cal}}^P \quad \dots\dots\dots\dots\dots\dots\dots\dots\dots\dots\dots\dots\dots\dots\dots\dots\dots \quad (2.16)$$

We can use above definition in Kalman Update equation and rewrite the equation. One of the advantages of the EnKF is that C^P is not necessary to compute fully. Since it is multiplied by the operator H, only some elements are needed to compute and store. For EnKF calculation, the cross covariance matrices $C^P H^T$ and $HC^P H^T$ are computed as follows:

$$C_k^P H^T = \frac{1}{N_e - 1} \sum_{j=1}^{N_e} (y_{k,i}^P - \bar{y}_k^P)[H(y_{k,j}^P - \bar{y}_k^P)]^T \quad \text{.........................} \quad (2.17)$$

$$HC_k^P H^T = \frac{1}{N_e - 1} \sum_{j=1}^{N_e} (Hy_{k,i}^P - H\bar{y}_k^P)[H(y_{k,j}^P - \bar{y}_k^P)]^T \quad \text{.....................} \quad (2.18)$$

Combined with Kalman Gain Equation, we can get complete version of EnKF update equation as follows:

$$K_k = C_k^P H_k^T (H_k C_k^P H_k^T + C_{D,k})^{-1} \quad \text{.........................} \quad (2.19)$$

$$y_k^u = y_k^P + C_k^P H_k^T (H_k C_k^P H_k^T + C_{D,k})^{-1} \left(d_{obs,k} - H_k y_k^P \right)$$

$$\text{.........................} \quad (2.20)$$

In summary, EnKF is able to sequentially update reservoir simulation models in a real time fashion as new observation data becomes available. This is very time efficient and suitable for frequent data integration and for large reservoir model. In aadition, EnKF is very applicable to implement in history matching work frame. For example, it is relatively easy to combine with any forward simulators because the EnKF is independent from forward simulation. What we need is output from simulator to update the reservoir models. And it can integrate many kinds of observation data such as water cut, bottom hole

pressure, Gas-Oil ratio and flowing rate, seismic data based on a statistical correlations. And finally, this is an ensemble model updating method which is associated with multiple models or ensemble of models .So we can easily analyze the uncertainty for future forecasts in updated models.

There are also disadvantages associated with EnKF. One is the Gaussian approximation applied in the update step. In some cases, such assumption may lead to unphysical and inconsistent results. Particularly, it is very difficult to perfectly implement EnKF for strong non-Gaussian problems. Secondly, repeated restarting followed by each update step is another disadvantage. This takes time to access and store restart file, reservoir simulator may start with unphysical and inconsistent reservoir model, especially for strong non-Gaussian problems. Ensemble Smoother with Multiple Data Assimilation (ES-MDA) is a viable alternative to EnKF and is introduced in the following section.

Mathematical Formulations for Ensemble Smoother

The state vector in Ensemble Smoother is

$$y_k = \begin{Bmatrix} m_k^{\mathbf{sta}} \\ \\ d_k^{cal} \end{Bmatrix} \qquad \ldots\ldots\ldots\ldots\ldots\ldots\ldots\ldots\ldots\ldots\ldots\ldots\ldots\ldots \text{ (2.21)}$$

The state vector in Ensemble Smoother (ES) is defined as joint state from time zero to time k:

$$\tilde{y} = \left\{ \begin{array}{c} y_k(t_0) \\ \vdots \\ y_k(t_k) \end{array} \right\} \quad \text{..} \quad (2.22)$$

ES is three dimensional matrix of state vector from time zero to time k instead of two dimensional EnKF state vector.

The ES covariance matrix of the state vector is represented as:

$$\tilde{C}_k^P = \frac{1}{N_e - 1} \sum_{j=1}^{N_e} (\tilde{y}_{k,i}^P - \bar{\tilde{y}}_k^P)(\tilde{y}_{k,j}^P - \bar{\tilde{y}}_k^P)^T \quad \text{...................} \quad (2.23)$$

As a linear variance to minimize ensemble smoother analysis, the following ES update scheme is proposed by Van Leeuwen and Evensen (1996). The linear update equation for ES is defined as:

$$\tilde{y}_k^u = \tilde{y}_k^P + \tilde{C}_k^P \tilde{H}_k^T (\tilde{H}_k \tilde{C}_k^P \tilde{H}_k^T + \tilde{C}_{D,k})^{-1} \tilde{D}' \quad \text{..............} \quad (2.24)$$

Where $\quad \tilde{D}' = \left(\begin{array}{c} D_1' \\ \vdots \\ D_m' \end{array} \right)' \quad \text{..} \quad (2.25)$

$$D' = \left(d_{obs,k} - H_k y_k^P \right) \quad \text{.......................................} \quad (2.26)$$

$$\tilde{H}_k = \left(\begin{array}{c} H_{k,1} \\ \vdots \\ H_{k,m} \end{array} \right) \quad \text{..} \quad (2.27)$$

$$\tilde{C}_{D,k} = \left(\begin{array}{ccc} C_{D,k}(t_1) & & \\ & \ddots & \\ & & C_{D,k}(t_m) \end{array} \right) \quad \text{...........................} \quad (2.28)$$

M is the subscript relating the total number of measurement time data available. Matrix D is an ensemble of perturbed observations data, which is same as EnKF. The data noise is assumed to be normally distributed with mean zero same as EnKF. It is clear that the ensemble of all observation time points are updated and can be treated as combination of forecast ensemble members from time zero to time k.
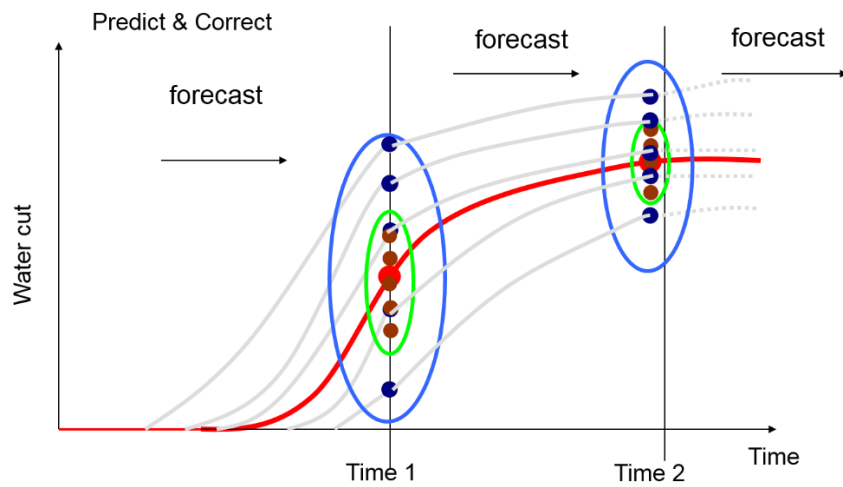
Figure 2: Flow diagram for Ensemble Smoother update process

Figure 2 is basic flow chart to illustrate how Ensemble Smoother works. We run all the ensemble from time zero to end time in forecast step and update each ensemble in update step.

Mathematical Formulations for Ensemble Smoother with Multiple Data Assimilation

In Emerick and Reynolds (2012), it is shown that applying ensemble smoother to assimilate data N_a times with the measurement errors covariance matrix multiplied by N_a is equivalent to assimilating the same data set only once with the original measurement errors covariance matrix for the linear- Gaussian case. Emerick and Reynolds (2012) showed that the updated mean and covariance obtained with MDA corresponds to the same posterior mean and covariance obtained assimilating data only once with the actual covariance of the measurement errors, C_D. It was showed that after data assimilation with MDA, the analyzed state vector is a sample of the correct posterior pdf. To obtain the correct posterior pdf for the linear-Gaussian case, observations covariance matrix was perturbed using larger measurement error with inflation coefficient α_i. Covariance of the measurement errors C_D can either be increased by a different coefficient α_i each time we assimilate data or we use the coefficients α_i's which satisfy

$$\sum_{i=1}^{N_a} \frac{1}{\alpha_i} = 1 \quad \dots\dots\dots\dots\dots\dots\dots\dots\dots\dots\dots\dots\dots\dots\dots\dots\dots\dots\dots \text{(2.29)}$$

This condition is required to guarantee the equivalence between single and multiple data assimilation.

For the nonlinear case, this equivalence does not hold. The motivation for using MDA in the nonlinear case comes from the fact that ES is equivalent to a single Gauss–Newton

iteration with a full step and an average sensitivity estimated from the prior ensemble

(Reynolds etal., 2006). In this sense, MDA can be interpreted as an ''iterative'' ensemble

smoother (with a predefined number of iterations), where instead of a single and

potentially large Gauss–Newton correction, we perform multiple smaller corrections in

the ensemble. Note that inflating the covariance matrix associated with the measurement

errors to damp the changes in the model at early iterations of Newton-like methods is not

new in the reservoir history-matching literature; see, e.g., Wu etal. (1999) and Gao and

Reynolds (2006).

The ES-MDA algorithm follows:

1. Choose the number of data assimilations N_a and the coefficients α_i for $i = 1,.. , N_a$

2. For $I = 1$ to N_a:

(a) Run the ensemble from time zero.

(b) For each ensemble member, perturb the observation vector using inflation coefficient

$$d_{k,i} = d_k + \sqrt{N_a}\,\varepsilon_i \quad \text{……....…...…...…..….....….....…...…….....………} \quad (2.30)$$

(c) Update the ensemble equation 2.24 using with $\tilde{C}_{D,k}$ replaced by $\alpha_i\,\tilde{C}_{D,k}$.

$$\tilde{y}_k^u = \tilde{y}_k^P + \tilde{C}_k^P\,\tilde{H}_k^T (\tilde{H}_k\,\tilde{C}_k^P\,\tilde{H}_k^T + \alpha_i\,\tilde{C}_{D,k})^{-1}\,\tilde{D}' \quad \text{…..….…} \quad (2.31)$$

$$C = \tilde{H}_k\,\tilde{C}_k^P\,\tilde{H}_k^T + \alpha_i\,\tilde{C}_{D,k} \quad \text{…………………….…....……….……} \quad (2.32)$$

As noted in Emerick and Reynolds (2012), the equivalence between single and multiple

data assimilation for the linear case by assimilating data N_a times simultaneously is

proved. However, in the MDA procedure presented above, we assimilate data N_a times consecutively and, before each data assimilation, we rerun the ensemble. For the linear-Gaussian case, these two approaches are equivalent. For the nonlinear case, these runs effectively serve to update the ''average sensitivity'' before the next data assimilation. Also note that in the ES-MDA algorithm, every time we repeat the data assimilation, we sample the vector of perturbed observation. This procedure tends to reduce sampling problems caused by matching outliers that may be generated when perturbing the observations.

One potential difficultly with the proposed MDA procedure is that N_a and the coefficients α_i's need to be selected prior to the data assimilation. The simplest choice is $\alpha_i = N_a$ for all i. However, intuitively we expect that choosing α_i in a decreasing order can improve the performance of the method. In this case, we start assimilating data with a large value of α_i, which reduces the magnitude of the initial updates; then, we gradually decrease α_i. We will test different number of data assimilation and α_i in a decreasing order in Chapter V.

As in Emerick and Reynolds (2012), EnKF with multiple data assimilation only shows little history matching improvement over standard EnKF while its computational efficiency is not as good as standard EnKF. In this thesis, we discuss about Ensemble Smoother with multiple data assimilation instead of EnKF with multiple data assimilation.

The first part of Chapter III consist of comparison of standard EnKF, single ensemble smoother and ES-MDA with all α_i equal to the number of data assimilation. In the second part we will run sensitivity analysis with different number of data assimilation and α_i in a decreasing order for each round of data assimilation. In both parts three ensemble methods are applied to a nine spot synthetic case and the Goldsmith field case. The default covariance localization method is distance based localization. Chapter IV will include history matching performance comparison for different localization methods applied to ES-MDA.

CHAPTER III

APPLICATION FOR ENSEMBLE KALMAN FILTER AND

ENSEMBLE SMOOTHER WITH MULTIPLE DATA

ASSIMILATION

Nine Spot Synthetic Case Application

A heterogeneous reference synthetic model was generated by sequential Gaussian simulation. The reservoir model is discretized into 51*51*1 grid blocks including one injector and eight producers as nine spot well pattern. The total simulation time is 2000 days with observation data of water-cut, bottom-hole pressure and gas-oil ratio. The data assimilation step is 200 days intervals for a total of 10 times. The preliminary synthetic field to be discussed in the following sections has the following specifications and EnKF parameters:

- High heterogeneity of permeability

- 51x51x1 grid system simulating 1530 ft X 1530 ft reservoir field.

- 9-Spot: 8 producers and 1 injector for water-cut matching

- Unfavorable mobility ratio with oil viscosity : 1.6 cp and water viscosity : 0.8 cp

- 1 Injection Rate at 200 RESV and, 8 Production rates at 50 RESV each

- Forward simulation is from 0 day to 2000 days

- Number of ensemble members: 60

- Water-cut/Bottom-hole pressure/Gas-oil ratio measurements

Three cases implemented for comparison are listed below:

Case1: EnKF 2000days, 10 sequential assimilations, number of realization is 60

Case2: ES-MDA 2000days, 1 assimilation, number of realization is 60

Case3: ES-MDA 2000days, 4 multiple assimilations, number of realization is 60

For ES-MDA, all α_i equal to the number of data assimilation, in this case we choose Na=4. Three ensemble methods are applied to nine spot synthetic case and the default covariance localization method is distance base localization. Mean permeability field for initial model, EnKF and ES-MDA are compared with true case. Ensemble realizations of permeability fields and permeability variance for EnKF and ES-MDA are compared. History matching performance in terms of water-cut, bottom-hole pressure and gas-oil ratio are compared. Root mean square errors for history matching, computational costs for EnKF and ES-MDA are calculated for comparison.
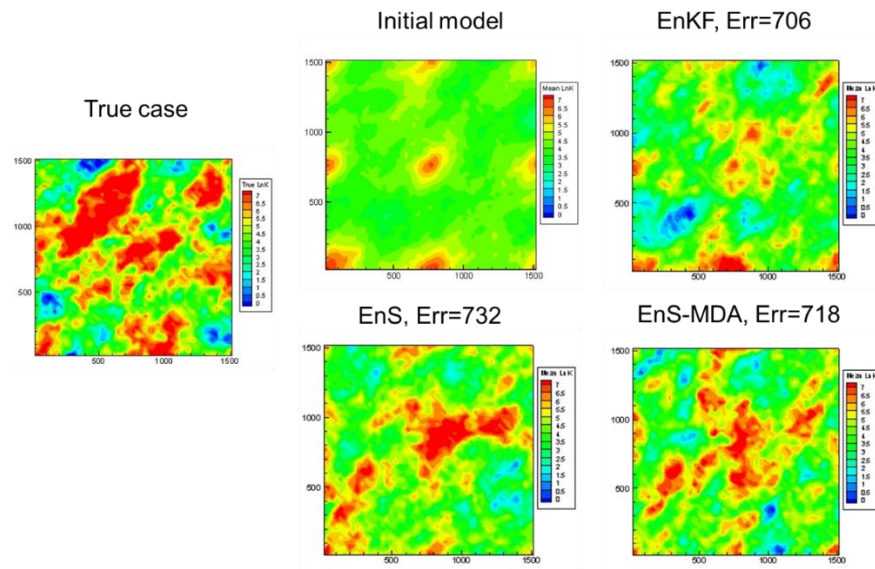
Figure 3 Updated ensemble mean permeability fields; from the left is true case, left top is initial model, right top is EnKF, left bottom is single ES, right bottom is ES-MDA. The error number associated with each permeability field is RMS errors.

In terms of the permeability field, Figure 2 shows that the mean of the ensemble permeability field and a comparison between initial mean model and the final updated model. The initial model is nine spot with permeability spread in the corner. The EnKF model has sequentially updated permeability field and shown significant improvement against initial model. EnKF capture permeability in the bottom part of true case. However the middle part and top part permeability field are not well represented. For ES permeability update, it capture part of middle permeability field of true case, however e top and bottom part are missing. On the other hand, ES-MDA has shown similar performance with ES. Diagonal permeability trend are well represented and the top part permeability field are partially captured.

26

In order to help quantity the history matching quality, the root mean square (RMS) is used as a measure to see how well overall the ensemble of computed responses are capturing the observed data. The RMS error is defined as:

$$RMS = \sqrt{\frac{1}{N_e}\sum_{i=1}^{N_e}(d_{cal,i} - d_{obs})^2} \quad \text{.. (3.1)}$$

Where Ne is the number of ensemble members, dcal, i is the computed dynamic response by each of the ensemble members, dobs is the observed data at the particular well, k is the assimilation time step.

The RMS is computed at each assimilation time step. The RMS errors referred to in the later water-cut history matching results are computed by summing the RMS computed through the assimilation time. In general, the smaller the RMS error, the closer are the ensemble computed responses to the observed data.

Table 1: Root Mean Square errors for EnKF, ES and ES-MDA, Unit: mD

Case	EnKF	ES	ES-MDA
RMS	706	732	718

As shown in Table 1, EnKF has the smallest RMS error compared with ES and ES-MDA. ES-MDA shows similar result with EnKF and single ES update has the largest RMS error.
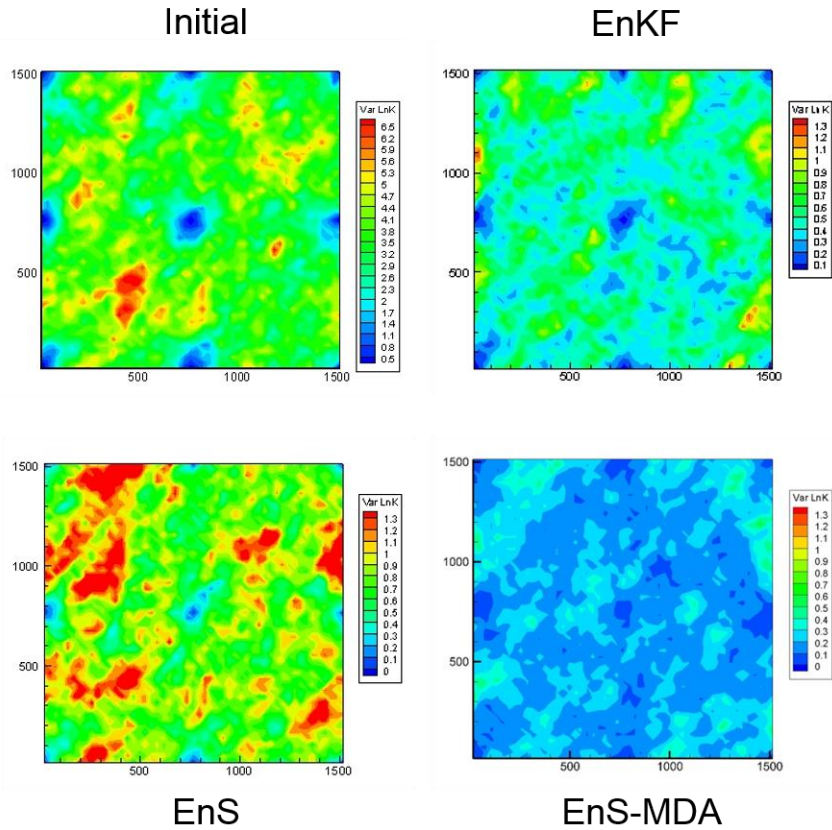
Figure 4: Updated ensemble permeability variance; left top is initial model, right top is EnKF, left bottom is single ES, right bottom is ES-MDA.

Other than updated permeability field, permeability variance between each ensembles are important to identify the permeability differences between updated permeability fields of each ensemble. As is shown in Figure 3, the permeability variance of ES-MDA has smaller value of EnKF, which means that for ES-MDA permeability update of each ensemble is quite similar to each other, this may cause potential ensemble collapse problem in the

application. To mitigate this problem, different number of data assimilation N_a and inflation coefficient α_i, different covariance localization methods for ES-MDA are tested in order to mitigate such ensemble collapse. Different number of data assimilation N_a and inflation coefficient α_i are tested in Chapter IV. Covariance localization methods will be discussed in Chapter V. The default covariance localization method here is distance base localization.

To better understand individual ensemble update, sample updated permeability field of EnKF and ES-MDA are shown below in Figure 4.
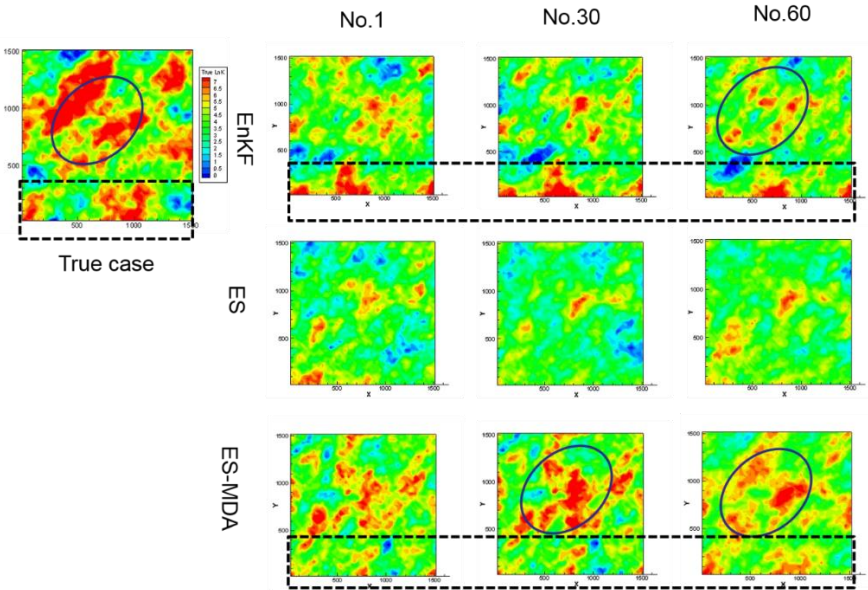
Figure 5: Sample updated permeability field of EnKF, ES and ES-MDA

Compare with Figure 3, Figure 5 shows updated permeability field from individual ensemble. It is consistent with variance permeability figure that ES-MDA permeability update of each ensemble is more similar to each other than EnKF. In the following section, water-cut history matching results for these ensemble methods implemented on producers P4, P5, and P7 among the eleven wells will be shown. We denote the conventional EnKF and EnKF, single ensemble smoother as ES and ensemble smoother with multiple data assimilation as ES-MDA.
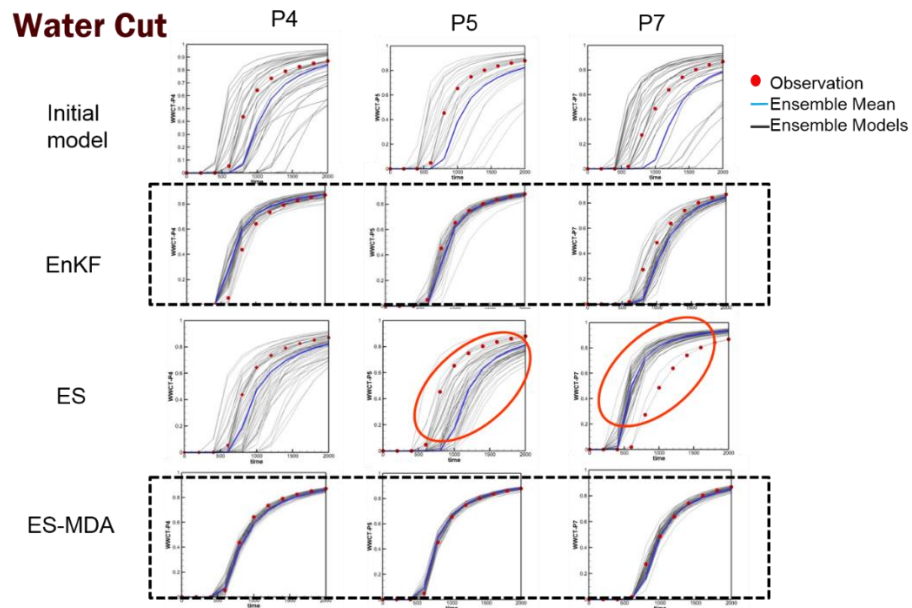
Figure 6: The EnKF and ES-MDA water-cut history matching results of producer 4, 5 and 7 for the total assimilation time of 2000 days. The first row is initial model response, second row is EnKF history match, third row is ES history match and last row is ES-MDA history match. Red dots dictates the reference model response while blue line dictates the mean of the ensemble responses.

From water-cut history matching results in Figure 6, the plots in first rows are from initial model history match, second row plots are EnKF history match and third row plots are single ES history match. The grey lines represent each ensemble result, blue line dictates the mean of the ensemble responses and red dots are the reference model response. It is clear that EnKF has significantly improve history match results compared with single ensemble smoother (ES). For single ensemble smoother (ES), significant divergence between mean of ensemble responses and reference model. Multiple data assimilation has improved the history matching performance compared with single ensemble smoother (ES). The ES-MDA has shown reduced spread in model responses from initial model and no systematic bias for history matching period. In terms of comparison between EnKF and ES-MDA, ES-MDA has lower RMS error and better history matching while EnKF has a wide spread to capture the reference model response.

In the following section, gas oil ratio (GOR) history matching results for these ensemble methods implemented on producers P4, P5, and P7 is shown in Figure 7.
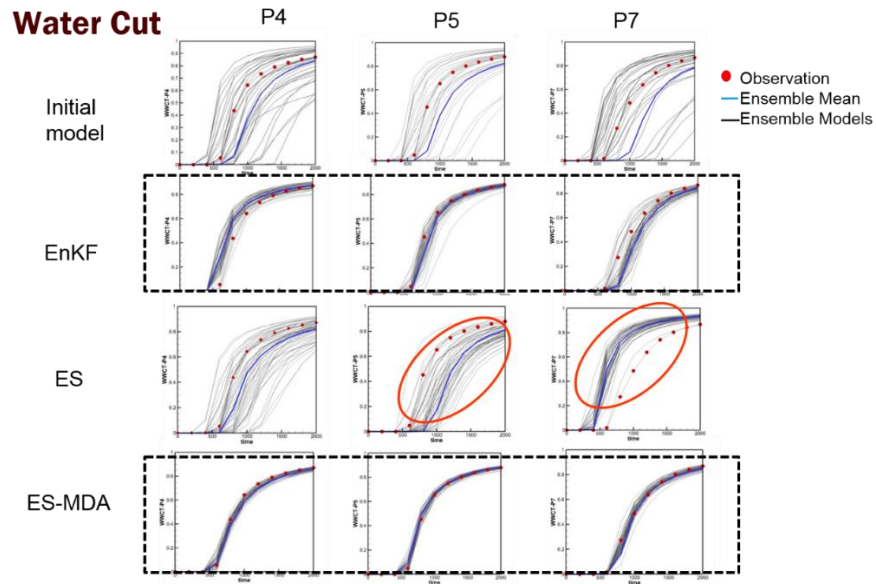
Figure 7: The EnKF and ES-MDA gas oil ratio (GOR) history matching results of producer 4, 5 and 7 for the total assimilation time of 2000 days. The first row is initial model response, second row is EnKF history match, third row is ES history match and last row is ES-MDA history match. Red dots dictates the reference model response while blue line dictates the mean of the ensemble responses.

In the following section, bottom-hole history matching results for these localization schemes implemented on producers P1, P2, and P3 among the nine wells is shown in Figure 8.
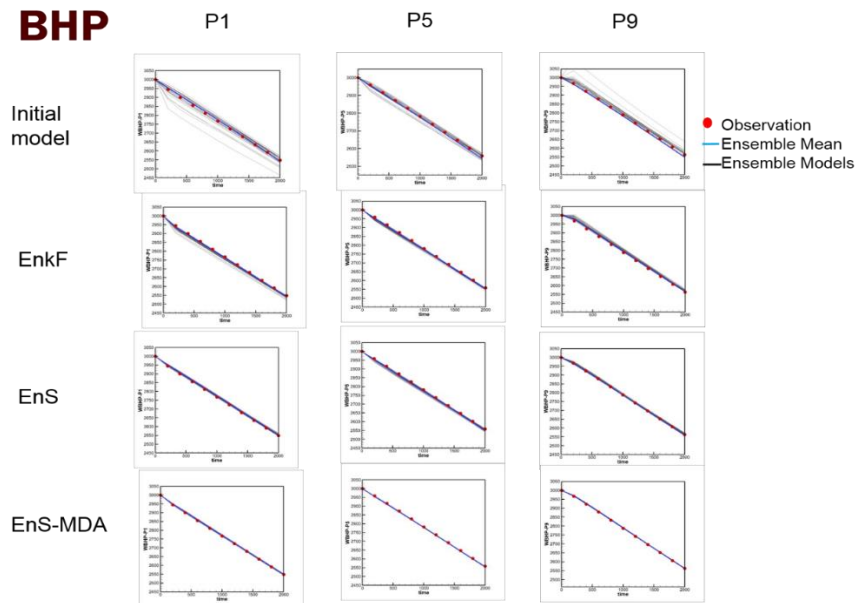
Figure 8: The EnKF and ES-MDA bottom-hole pressure (BHP) history matching results of producer 4, 5 and 7 for the total assimilation time of 2000 days. The first row is initial model response, second row is EnKF history match, third row is ES history match and last row is ES-MDA history match. Red dots dictates the reference model response while blue line dictates the mean of the ensemble responses.

In Table 2, we show that the root mean square (RMS) error for history matching of water-cut, gas oil ratio (GOR) and bottom-hole pressure (BHP). It is consistent with history matching plots that ES-MDA has a relatively better history matching quality compared with EnKF and has a significant improvement against single ensemble smoother (ES).

Table 2: The EnKF and ES-MDA RMS error of history matching for the total assimilation time of 2000 days. The first column is initial model response, second column is EnKF history match, third column is ES history match and last column is ES-MDA history match.

	Initial	EnKF	ES	ES-MDA
WCT	2.64E+03	1.72E+01	1.38E+02	1.01E+01
BHP	3.54E+07	4.14E+06	1.45E+07	1.89E+06
GOR	1.11E+03	5.87	8.11	3.55

In Table 3, we show that the computation time for EnKF, ES and ES-MDA in synthetic case history matching. For synthetic case ES-MDA only consume one third time of EnKF and has shown great computational efficiency. This is also main advantage of ES-MDA against EnKF. On the other hand single ensemble smoother (ES) has shortest computation time among these ensemble methods. Depend on the number of data assimilations applied in ES-MDA, single ensemble smoother (ES) normally can generate less accurate history matching result with fastest computation time. In some case, single ensemble smoother (ES) is also acceptable for history matching and prediction.

Table 3: The EnKF and ES-MDA water-cut matching results of each of the three producers for the total assimilation time of 2000 days.

Case	EnKF	ES	ES-MDA
Computation time (sec.)	3.201E+03	4.441E+02	1.106E+03

In terms of compassion between EnKF and ES-MDA, ES-MDA is able to generate good history matching performance, which is comparable and sometimes even better than EnKF, but ES-MDA has greater computation efficiency over EnKF. The above statement will further be verified in field case in the following chapter. The potential disadvantage of ES-MDA is ensemble collapse problem in this application. To mitigate this problem, covariance localization methods are utilized to avoid such ensemble collapse in the following chapters.

Goldsmith Case Application

To further evaluate and compare performance of EnKF and ES-MDA, these methods are applied to a large and complex Goldsmith field case study. The simulation model has dimensions of 58 by 53 by 10 in a corner point grid system. The production area comprises of nine 5-spot patterns covering around 320 acres. The total number of wells is 44 with 11 injectors and 33 producers. Water-cut data for 20 years of production prior to the start of the CO_2 flood is available at 9 production wells and these were used to condition the permeability fields. The total simulation time is 7800days with observation data of water-cut. The data assimilation step is 390 days intervals for a total of 20 times. The number of ensemble in EnKF is 50. Description of the EnKF/ES-MDA parameters for this case is given below:

- 58 x 53 x 10 (5836 ft x 5333 ft x 87ft)

- Oil-Water-Gas 3 Phase

- 44 spot waterflooding 11 Injector / 33 producers

- Water-cut measurements

- History matching period: 7800days

- The number of the ensemble is 50

Three cases implemented for comparison are listed below:

Case1: EnKF 7800days, 10 sequential assimilations, number of realization is 50

Case2: ES-MDA 7800days, 1 assimilation, number of realization is 50

Case3: ES-MDA 7800days, 4 multiple assimilations, number of realization is 50

We will discuss about application of EnKF and ES-MDA to a real field case. The so called Goldsmith field case shown in Figure 9 is from the Gold Smith San Andres Unit GSAU, a dolomite formation in west Texas. A total of 7800 days, around 20 years of water flood production history are history matched. The pilot area consists of nine inverted five-spot patters covering approximately 320 acres with an average thickness of 100 ft.
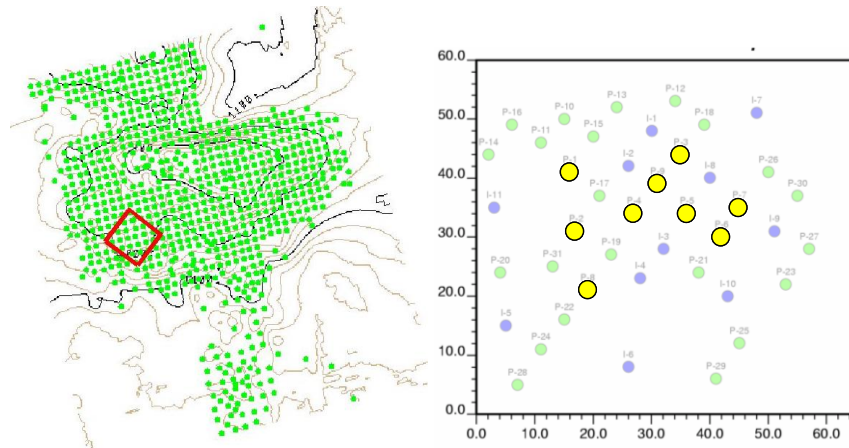
Figure 9: Goldsmith study area; well distribution producer with water cut information highlighted in yellow; Injectors in blue.

The area has more than 50 years of production history before the initiation of the CO_2 project in 1996. Due to practical difficulties describing the correct boundary conditions for the pilot area, wells around the pilot area were included in this study. The study area includes 11 injectors and 33 producers. Production history information from only 9 producers is used; since only these have significant water cut response. The detailed production rate and the well schedule, including infill drilling, well conversions, and well shut-in can be found elsewhere. The study area was discredited into 58x53x10 grid blocks. The initial 50 realizations of porosity and permeability were obtained using sequential Gaussian simulation conditioned to well and seismic data. Mean permeability field for initial model, EnKF and ES-MDA are compared. The real permeability field is unknown. Ensemble realizations of permeability fields and permeability variance for EnKF and ES-MDA are compared.

The problems posted by the EnKF while working with non-Gaussian permeability field becomes more evident in this field case. On the other hand an analysis of the ability of the updated members to match the observation reveals that the spread in the water cut of the initial members was greatly decreased around the observation although the permeability became totally unrealistic.

Due to the very high dimensionality of the problem and the small number of constraints: it is not surprising that in history matching it will be always possible to find a set of model parameters that satisfy the data but have a totally unrealistic description of the model parameters. This behavior demonstrates that judging the success of the EnKF and ES-MDA based on the ability of the final members to reproduce the history is incomplete; a detailed study of the final permeability field is in general recommended. Unfortunately for actual cases where the true permeability is unknown and this is not a trivial task.

In the present field case, the wells that contain water cut information are located towards the center of the model; injectors are located around the producers; this suggest that the flow of water arriving to each wells should most probably travel across the volume surrounded by the injectors and the wells; a small amount of water should be traveling close to the boundaries of the model were stagnation points can occurs; this ideas naturally lead to think that the majors changes proposed by ensemble methods should be preferentially found in the area subscribed by the injectors and wells with observations. However, in this particular example ensemble methods including EnKF and ES-MDA has

produced changes in all parts of the model indiscriminately of the wells and injector position.
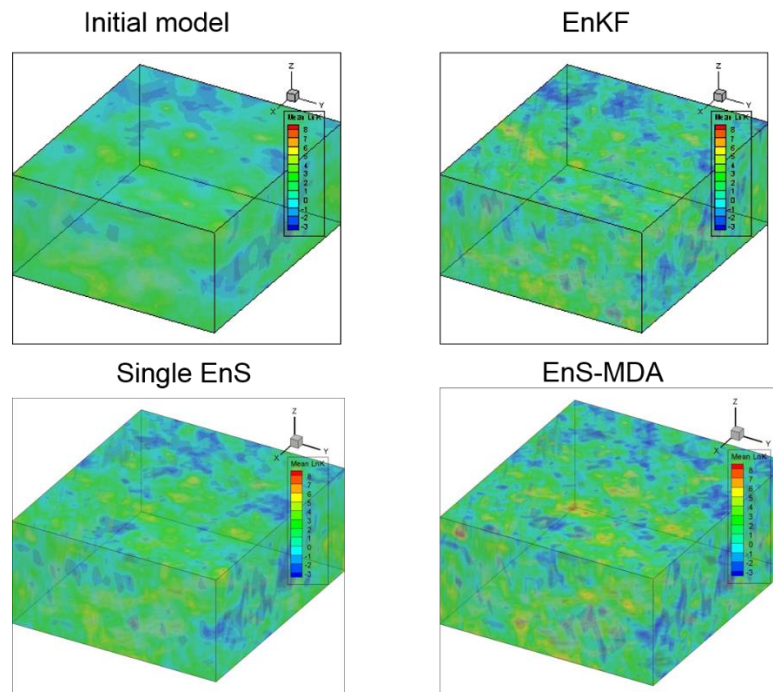
Figure 10: Updated ensemble mean permeability fields; left top is initial model, right top is EnKF, left bottom is single ES, right bottom is ES-MDA.

In terms of the permeability field, Figure 10 shows that the mean of the ensemble permeability field and a comparison between initial mean model and the final updated model. The EnKF and ES-MDA model has sequentially updated permeability field and shown significant improvement against initial model.
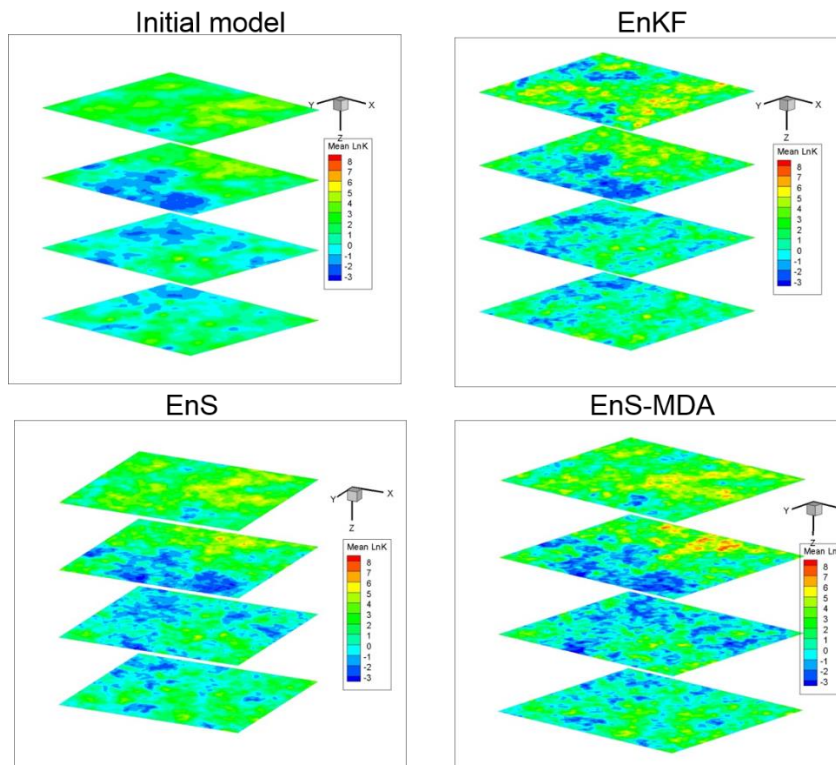
Figure 11: Layer view of updated ensemble mean permeability fields; left top is initial model, right top is EnKF, left bottom is single ES, right bottom is ES-MDA.

Figure 11 is layer view of updated ensemble mean permeability fields. Left top is initial model, right top is EnKF, left bottom is single ES and right bottom is ES-MDA. The four layers are layer one, layer four, layer seven and layer ten. The total layer in horizontal direction is ten. It clearly demonstrated that each layer has updated its permeability field over ensemble method data assimilation.
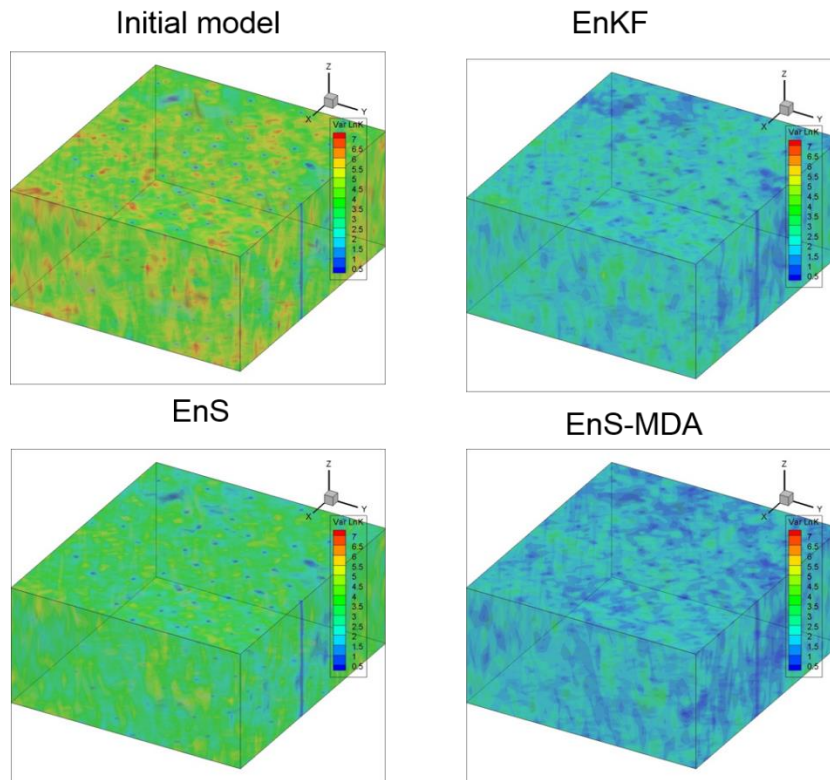
Figure 12: ensemble mean permeability fields; left top is initial model, right top is EnKF, left bottom is single ES, right bottom is ES-MDA.

Other than updated permeability field, permeability variance between each ensembles are important to identify the permeability differences between updated permeability fields of each ensemble. As is shown in Figure 12, it is expected the variance is small around the well position. A closer look of the variance maps, from both techniques, reveals that the in the overall there are more zones with small variance when using the ES-MDA that when using the standard EnKF. Although here we show the maps from the 60 ensemble members only similar results were obtained with ensembles size of 30 and 100 members. The permeability variance of ES-MDA has smaller value of EnKF, which means that for

ES-MDA permeability update of each ensemble is quite similar to each other, this may cause potential ensemble collapse problem in the application. To mitigate this problem, covariance localization methods are utilized to avoid such ensemble collapse. Covariance localization methods will be discussed in next chapter. The default covariance localization method here is distance base localization. To better understand individual ensemble update, ensemble permeability variance of EnKF and ES-MDA are shown below in Figure 13.
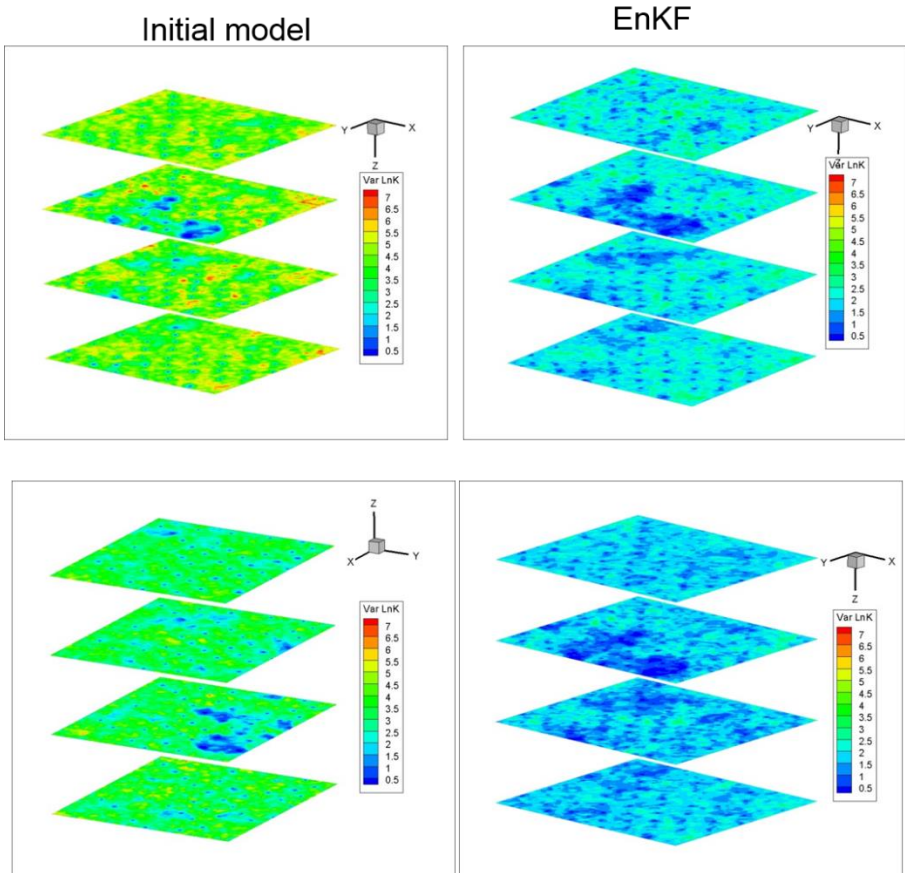

Figure 13: Layer view of updated ensemble permeability variance; left top is initial model, right top is EnKF, left bottom is single ES, right bottom is ES-MDA.

Figure 14 is the EnKF and ES-MDA water-cut history matching results of producer 1, 3 and 7 for the total assimilation time of 7800 days. The plots in first rows are from initial model history match, second row plots are EnKF history match and third row plots are single ES history match. The grey lines represent each ensemble result, blue line dictates the mean of the ensemble responses and red dots are the reference model response. It is clear that EnKF has significantly improve history match results compared with single ensemble smoother (ES). For single ensemble smoother (ES), significant divergence between mean of ensemble responses and reference model. Multiple data assimilation has improved the history matching performance compared with single ensemble smoother (ES). The ES-MDA has shown reduced spread in model responses from initial model and no systematic bias for history matching period. In terms of comparison between EnKF and ES-MDA, ES-MDA has lower RMS errors and better history matching while EnKF has a wide spread to capture the reference model response.
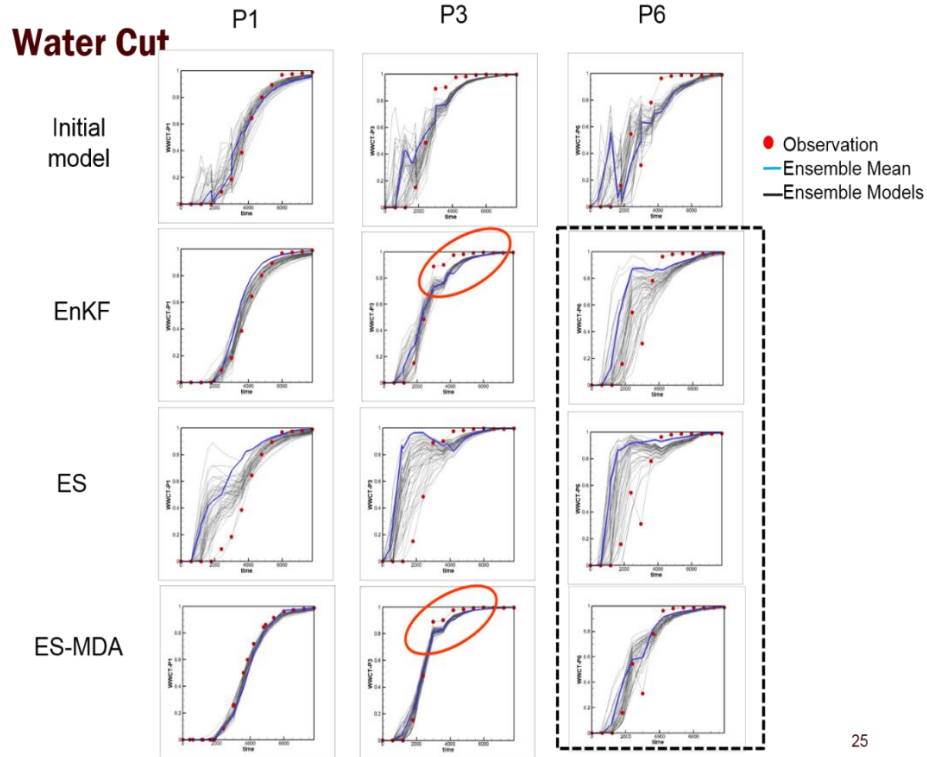
Figure 14: The EnKF and ES-MDA water-cut history matching results of producer 1, 3 and 7 for the total assimilation time of 7800 days. The first row is initial model response, second row is EnKF history match, third row is ES history match and last row is ES-MDA history match. Red dots dictates the reference model response while blue line dictates the mean of the ensemble responses.

Table 4: The EnKF and ES-MDA RMS error of water cut history matching for the total assimilation time of 7800 days.

	Initial	EnKF	ES	ES-MDA
WCT	5.22E+03	1.45E+02	6.14E+02	6.79E+01

In Table 4, we show that the root mean square (RMS) error for history matching of water-cut. It is consistent with history matching plots that ES-MDA has a relatively better

history matching quality compared with EnKF and has a significant improvement against single ensemble smoother (ES).

Table 5: Computational time comparison of the EnKF, ES and ES-MDA

Case	EnKF	ES	ES-MDA
Computation time (sec.)	2.426E+04	4.093E+03	1.042E+04

In Table 5, we show that the computation time for EnKF, ES and ES-MDA in Goldsmith case history matching. For synthetic case ES-MDA only consume half time of EnKF and has shown great computational efficiency. This is also main advantage of ES-MDA against EnKF. On the other hand single ensemble smoother (ES) has shortest computation time among these ensemble methods. Depend on the number of data assimilations applied in ES-MDA, single ensemble smoother (ES) normally can generate less accurate history matching result with fastest computation time. In some case, single ensemble smoother (ES) is also acceptable for history matching and prediction.

In terms of compassion between EnKF and ES-MDA, ES-MDA is able to generate good history matching performance, which is comparable and sometimes even better than EnKF, but ES-MDA is a much more effective option in terms of computational cost than ES-MDA.

CHAPTER IV

SENSITIVITY ANALYSIS FOR NUMBER OF DATA

ASSIMILATION AND INFLATION COEFFICIENT

In Chapter II, we discussed that one potential difficultly with the proposed MDA procedure is that N_a and the coefficients α_i 's need to be selected prior to the data assimilation. The simplest choice is $\alpha_i = N_a$ for all i. Covariance of the measurement errors C_D can either be increased by a different coefficient α_i, each time we assimilate data or we use the coefficients α_i 's which satisfy

$$\sum_{i=1}^{N_a} \frac{1}{\alpha_i} = 1 \qquad \text{.. (2.30)}$$

This condition is required to guarantee the equivalence between single and multiple data assimilation.

However, intuitively we expect that choosing α_i in a decreasing order can improve the performance of the method. In this case, we start assimilating data with a large value of a, which reduces the magnitude of the initial updates; then, we gradually decrease a. We will test different number of data assimilation and α_i in a decreasing order in this chapter.

Three cases implemented in Goldsmith case for comparison are listed below:
Case1: ES-MDA, 3 multiple assimilations, $\alpha_1 = \alpha_2 = \alpha_3 = 3$;

Case2: ES-MDA, 4 multiple assimilations, $\alpha_1 = \alpha_2 = \alpha_3 = \alpha_4 = 4$;

Case3: ES-MDA, 4 multiple assimilations, $\alpha_1 = \alpha_2 = 8, \alpha_3 = 4; \alpha_4 = 2$;

Figure 15 is ES-MDA water-cut history matching results of producer 1, 3 and 6 for the total assimilation time of 7800 days in Goldsmith case. The plots in first rows are from case 1 history match with three data assimilations; second row plots are case 2 history match with four data assimilations, same inflation coefficient; third row plots are case 3 history match with inflation coefficient in decreasing order. The grey lines represent each ensemble result, blue line dictates the mean of the ensemble responses and red dots are the reference model response. Comparing three data assimilations and four data assimilations, larger number of data assimilations has significantly improve history match results. Especially for P1, history match quality of three data assimilations is not as good as four data assimilations. Significant divergence between mean of ensemble responses and true history data is observed. Case 2 and 3 with four data assimilations have shown reduced spread in model responses from initial model and for 20 years history matching time no systematic bias is observed. For case 6, one abnormal history data at 3200 days is ignored.
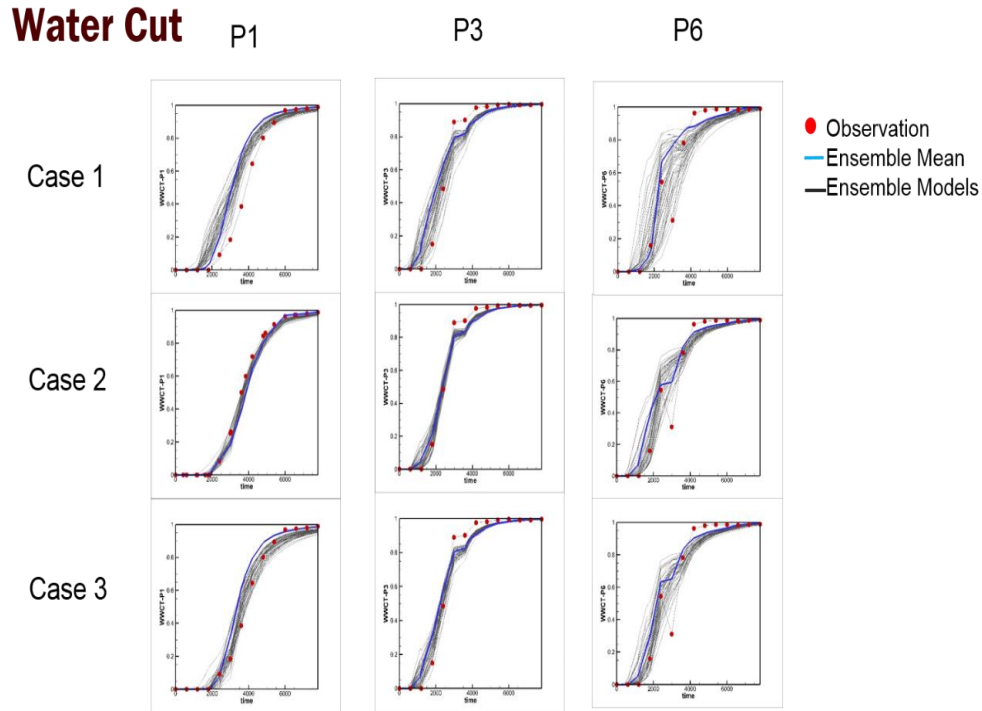
Figure 15: Water-cut history matching results of producer 1, 3 and 6 for the total assimilation time of 7800 days. The first rows are from case 1 history match with three data assimilations; second row plots are case 2 history match with four data assimilations, same inflation coefficient; third row plots are case 3 history match with inflation coefficient in decreasing order

Figure 16 is ensemble permeability variance results the total assimilation time of 7800 days in Goldsmith case. Case 2 with four data assimilations and same inflation coefficient has a potential ensemble collapse problem, however Case 1 and case 3 has retained good variability between each ensemble. With the increasing number of data assimilations, the variability is reduced. Choice of inflation coefficient also influence permeability variance with same data assimilations. Inflation coefficient in a decreasing order retain better variability than using same inflation coefficient.
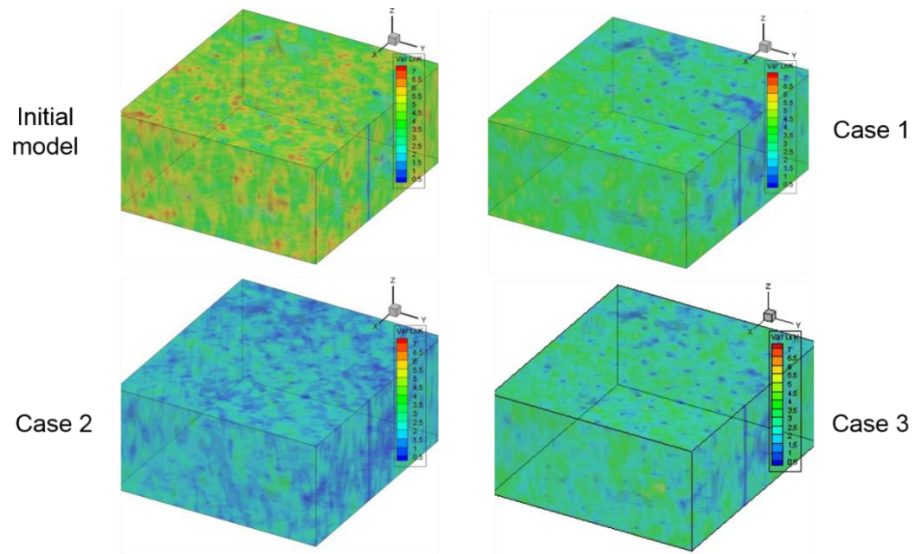
Figure 16: Ensemble permeability variance; left top is initial model, right top is case 1 history match with three data assimilation, left bottom is case 2 history match with four data assimilations, same inflation coefficient right bottom is case 3 history match with inflation coefficient in decreasing order

Table 6: Total Root Mean Square Errors for Goldsmith case ES-MDA case 1, 2 3 and EnKF

Case	1	2	3	EnKF
RMS	1.58E+02	6.79E+01	1.02E+02	1.45E+02

In Table 6, we show that the root mean square (RMS) errors for Goldsmith case history matching of water-cut. It is consistent with history matching plots that ES-MDA with four data assimilations has a relatively better history matching quality compared with standard EnKF and ES-MDA with three data assimilations. ES-MDA with three data assimilations has larger RMS error over standard EnKF. It shows that the history match quality

49

improves with larger number of data assimilations. Comparing case 2 and case 3, case 3 with inflation coefficients α_i in a decreasing order resulted in small performance improvements over same α_i for all assimilations.

Table 7: Computational time Goldsmith case ES-MDA case 1, 2 3 and EnKF

Case	1	2	3	EnKF
Time(sec)	8.21E+03	1.042E+04	1.15E+04	2.43E+04

In Table 7, we show that the computational cost for Goldsmith case history matching of water-cut. Case 1, 2 and 3 all have better computation efficiency over standard EnKF. It is as expected that case 1 with three data assimilations use least computational time. Case 2 and 3 using different inflation coefficients have close computational time.

Based on above observations, four data assimilations generally perform better than three data assimilations. Three data assimilations is also acceptable as it is a more effective option in terms of computational cost. Four data assimilations with inflation coefficients α_i in a decreasing order resulted in small performance improvements over case using same α_i. More cases should be carried out to compare history matching performance and computational time for different choice of inflation coefficients. Five data assimilation is recommended to test and it is expected to have good history matching quality and longer computational time.

CHAPTER V

MOTIVATION AND METHODOLOGY FOR COVARIANCE LOCALIZATION STUDY

Introduction to Covariance Localization Study

Three localization methods including distance based localization, streamline based localization and hierarchical ensemble filter localization are applied to both EnKF and ES-MDA for localization method history matching performance comparisons.

EnKF and ES-MDA are implemented in the 9-Spot synthetic field with the following schemes: (i) distance based covariance localization, (ii) streamline based covariance localization, and (iii) hierarchical covariance localization.

The theory and methodology of each localization scheme are summarized in the following sections. The history matching performance results are compared in order to find out best localization scheme to be implemented and for further research.

As mentioned in Chapter II, the state vector update equation for EnKF is:

$$y_k^u = y_k^P + C_k^P H_k^T (H_k C_k^P H_k^T + C_{D,k})^{-1}\left(d_{obs,k} - H_k y_k^P\right) \quad \text{.....................} (4.1)$$

While the Kalman Gain is:

$$K_k = C_k^P H_k^T (H_k C_k^P H_k^T + C_{D,k})^{-1} \qquad \ldots\ldots\ldots\ldots\ldots\ldots\ldots\ldots\ldots\ldots \text{(4.2)}$$

$\rho \circ$ is either the localization function or multiplier function, this is s specified parameter for covariance localization. It is introduced to modify the Kalman Gain during update step for both EnkF and ES-MDA. The symbol '$\circ$' is an element-by-element multiplication operator known as the Schur product (Gaspari and Cohn, 1996). The update equation with covariance localization is:

$$y_k^u = y_k^P + \rho \circ C_k^P H_k^T (H_k C_k^P H_k^T + C_{D,k})^{-1} \left(d_{obs,k} - H_k y_k^P \right) \qquad \ldots\ldots \ldots\ldots\ldots \text{(4.3)}$$

As mentioned in Chapter II, the cross covariance matrix is:

$$C^P H^T = \begin{pmatrix} C_{\mathbf{m}^{sta}} & C_{\mathbf{m}^{sta},\mathbf{m}^{dym}} & C_{\mathbf{m}^{sta},\mathbf{d}^{cal}} \\ C_{\mathbf{m}^{dym},\mathbf{d}^{cal}}^{\mathbf{T}} & C_{\mathbf{m}^{dym}} & C_{\mathbf{m}^{dym},\mathbf{d}^{cal}} \\ C_{\mathbf{m}^{sta},\mathbf{d}^{cal}}^{\mathbf{T}} & C_{\mathbf{m}^{dym},\mathbf{d}^{cal}}^{\mathbf{T}} & C_{\mathbf{d}^{cal}} \end{pmatrix}^P \begin{pmatrix} 0 \\ 0 \\ 1 \end{pmatrix} = \begin{pmatrix} C_{\mathbf{m}^{sta},\mathbf{d}^{cal}} \\ C_{\mathbf{m}^{dym},\mathbf{d}^{cal}} \\ C_{\mathbf{d}^{cal}} \end{pmatrix}^P \qquad \ldots\ldots \text{(4.4)}$$

Sub-matrix $C_{m^{sts},d^{cal}}$ in cross-covariance matrix is the main factor for update in the static parameters. $C_{m^{sts},d^{cal}}$ is able to capture the cross-covariance between the static parameters and observation data. In this thesis we are interested in static parameters including log permeability and water-cut, observation data bottom-hole pressure. The sub-matrix $C_{m^{sts},d^{cal}}$ is shown as the following:

$$C_{m^{sts},d^{cal}} = \begin{matrix} \text{cov}[\log(k_1),WBHP] & \text{cov}[\log(k_1),WWCT] \\ \vdots & \vdots \\ \text{cov}[\log(k_{N_{grid}}),WBHP] & \text{cov}[\log(k_{N_{grid}}),WBHP] \end{matrix} \qquad \ldots\ldots\ldots \text{(4.5)}$$

The main objective for three localization methods are to localize the cross covariance matrix. The localizing function are different for each localization schemes and localizing function used to modify the cross-covariance is computed at each observation data time. The final goal of the covariance localization methods is to eliminate erroneous terms in the cross-covariance matrix and preserve the underlying geology information from prior.

Distance Based Covariance Localization

The fluid production rate in the reservoir field including oil and water production rate has a non-linear relationship with reservoir grid block at large distance away. To better estimate the reservoir permeability, the relationship between the well of observation and grid block need to be well understood.

The computed cross-covariance between the permeability and fluid production rate can be overestimated due to their highly non-linear relationship especially when a smaller ensemble size is used (Hamill et al., 2001). It is commonly known as overshooting problem. Another problem is that small size ensemble member may not work well in estimating error covariance. Hamill et al. (2001) mentioned that we can improve the analysis scheme by excluding observations at large distances away from the grid point we are interested.

We use a fifth order function (Gaspari and Cohn, 1996). The set of equations used are as follows to define the covariance correlation:

$$\rho(a,b) = -\frac{1}{4}\left(\frac{b}{a}\right)^5 + \frac{1}{2}\left(\frac{b}{a}\right)^4 + \frac{5}{8}\left(\frac{b}{a}\right)^3 - \frac{5}{3}\left(\frac{b}{a}\right)^2 \quad................................,0 \le b \le a;$$

$$\rho(a,b) = \frac{1}{12}\left(\frac{b}{a}\right)^5 - \frac{1}{2}\left(\frac{b}{a}\right)^4 + \frac{5}{8}\left(\frac{b}{a}\right)^3 + \frac{5}{3}\left(\frac{b}{a}\right)^2 - 5\left(\frac{b}{a}\right) + 4 - \frac{2}{3}\left(\frac{b}{a}\right)^{-1},a < b \le 2a; \quad .. (4.6)$$

$$\rho(a,b) = 0 ....,b > 2a.$$

Where b is the distance between the well location (observation point) and the grid point underlying the model parameters, where a is the multiplication of the factor of $\sqrt{10/3}$ and the length scale l_c:

$$a = \sqrt{10/3} l_c \qquad .... (4.7)$$

$$\text{or } F_c = \sqrt{10/3} l_c, \text{ since } a = F_c \qquad .... (4.8)$$

A correlation matrix S is defined for every grid point (i,j) in the domain:

$$S(i, j) = \Omega(F_c, \|D_{ij}\|) \qquad .... (4.9)$$

D_{ij} denotes the Euclidean distance between grid point (i,j) and the location of observation (Hamill, Whitaker et al. 2001). From the above equations, we know that the multiplier is in a decreasing order from the observation location to the grid blocks at long distances. The multiplier value is 1 at the observation locations and 0 asymptotically at grid blocks of long distance away from the wells. The cut off radius is the place where multiple value become zero. Therefore, the localizing function is composed of a matrix with 0's and 1's. This lead to a weighting effect for model parameters update and reduce erroneous information from observation data at large distance away from observation location.

The default localization method used for synthetic case is distance based localization. Goldsmith field has a size of 1530 ft x 1530 ft and the cut off radius used is 900 ft.

Streamline Based Covariance Localization

Streamline base covariance localization is another approach to identify the zones where there is significant impact for state parameters and data observations are closely correlated. Streamline base covariance localization utilize prior information of the governing physical phenomena to identify impact zones.

Accord to Arroyo, he grid blocks intersected by a streamline originated from the observation location is identified as impact zones which is closely correlated with data observation. Only the terms related to the grid blocks intersected by streamline will be retained within covariance matrix calculation for each observation data (Arroyo et al. 2006). For this study, the observation data is water cut.

The covariance matrix term $C_{m^{sts},d^{cal}}$ is shown in the following:

$$C_{m^{sts},d^{cal}} = \begin{matrix} \mathrm{cov}[\log(k_1),WBHP] & \mathrm{cov}[\log(k_1),WWCT] \\ \vdots & \vdots \\ \mathrm{cov}[\log(k_{N_{grid}}),WBHP] & \mathrm{cov}[\log(k_{N_{grid}}),WBHP] \end{matrix} \qquad \ldots\ldots\ldots\ldots (4.10)$$

The water swept zones is identified at different time-of-flight values with aid of streamlines. The ensemble covariance conditioned by the streamline is able to deduce zones where the production data and the parameters are closely correlated (Emanuel and Milliken 1998). The rest of matrix term is defined to be zero. Streamline base localization is able to reduce erroneous information from observation data where state parameters and data observations are not closely correlated.

Hierarchical Based Covariance Localization

Hierarchical base covariance localization is proposed by Anderson to split the initial members into groups of members. The procedures of implementing

The implementation of Hierarchical base covariance localization follows the procedures (Anderson 2004):

i)   Divide the initial realizations into m groups of n-member ensembles (total 'm x n' members). The multiplier ρ is calculated by minimizing the following equation:

$$\rho_{min} = \sqrt{\sum_{j=1}^{m} \sum_{i=1,i\neq j}^{m} (\alpha\beta_i - \beta_j)^2}$$ .... (4.12)

β is the regression factor for the ith group (i.e. i = 1,…, m). The following equation is utilized to minimize the weighting factor:

$$\alpha_{min} = max\left[\frac{m-Q^2}{(m-1)Q^2+m}, 0\right]$$ .... (4.13)

ii)   The *n* ensemble members within each group are same as standard Ensemble

Kalman Filter except linear regression is applied in update step for each ensemble. The

linear regression in update step is calculated for each ensemble by multiplying the sample

regression coefficient β_i by the regression confidence factor Q. Q is defined in the

following equation:

$$Q = \frac{\sqrt{\sum_{i=1}^{m}\left(\beta_i^{k,obs} - \overline{\beta}^{k,obs}\right)^2 \Big/ m-1}}{\overline{\beta}^{k,obs}} \qquad \text{.......................... (4.14)}$$

Where $\overline{\beta}^{k,obs} = \sum_{i=1}^{m} \beta_i^{k,obs} \Big/ m$ $\qquad$ .... (4.15)

For Hierarchal based localization, we group initial 50 ensemble members to 2 groups of

25 members.

Covariance Localization Data Assimilation Results Comparison

In this study, three covariance localization schemes are implemented in the Goldsmith

case based on the assumption that the model parameters and observation data are closely

related within a certain cut-off radius.

The cut-off radius is chosen manually and its performance is tested by history matching

quality comparison. Hamill and Whitaker (2001) observed that the length scale used to

achieve covariance localization is a function of the ensemble size. The problem is how to

choose best cut-off radius is still unknown; however, we can take advantage of initial

geological knowledge to assist in cut-off radius selection. It still require trial-and-error in order to achieve best results. In addition, different covariance localization schemes may not be consistent with the underlying heterogeneity that include high permeability channels with long-range contributions (Arroyo et al. 2006).

In this study, the preliminary pick for the cut-off radius is 900ft, in comparison to the nine spot model with dimensions of 1530 ft x 1530 ft. Distance covariance localization should gain reasonable results as long as the appropriate length scale is used. For Hierarchal localization, we group initial 50 ensemble members to 2 groups of 25 members. In order to examine the quality of the distance-based covariance localization scheme in more dimensions, RMS errors of the updated permeability with respect to the reference model permeability through the assimilation time are examined.
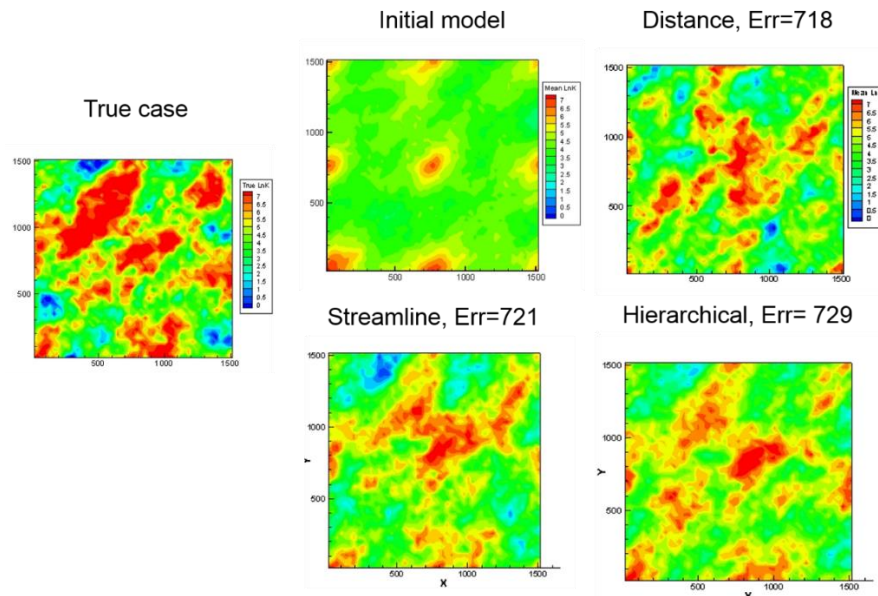
Figure 17: Mean permeability field for distance based, streamline and hierarchical localization methods

In terms of the permeability field, Figure 17 shows that the mean of the ensemble permeability field and a comparison between initial mean model and the final updated model for three localization methods. The initial model is nine spot with permeability spread in the corner. For all three localization schemes, the updated mean permeability field are very similar to each other. They all capture part of middle permeability field of true case, however top and bottom part are missing.
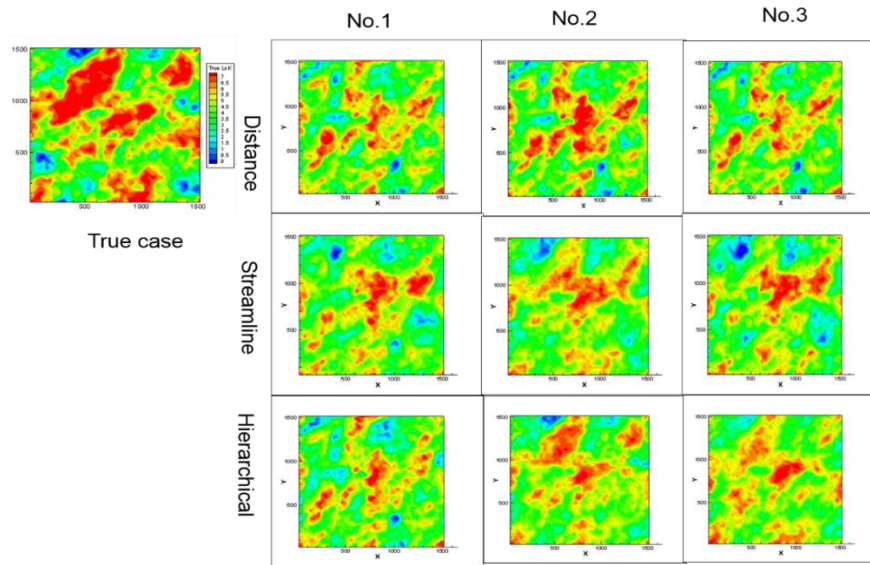
Figure 18: Sample ensemble of updated permeability field for three localization methods

To better understand individual ensemble update, sample updated permeability field of three localization methods are shown below in Figure 18. In Figure 19, we compare the performance of history matching for three localization methods: P4 water cut history matching, P5 bottom-hole pressure history matching and P4 gas oil ratio history matching. Table 8 lists the RMS errors for water cut, bottom-hole pressure and gas oil ratio history matching of three localization methods.
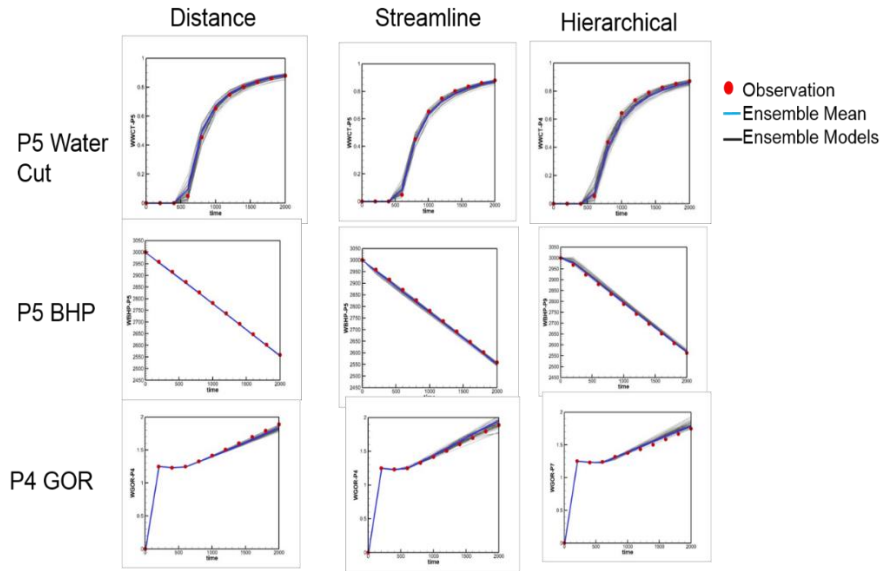
Figure 19: History matching performance comparison for three localization methods.

Table 8: RMS errors for three localization methods in history matching

	Distance	Streamline	Hierarchical	EnKF
WCT	1.61E+01	1.22E+01	1.77E+01	1.72E+01
BHP	1.89E+06	2.45E+06	3.03E+06	4.14E+06
GOR	3.55	3.69	4.22	5.87

From the results obtained above in Table 8, the performance between three localization methods are of small difference. Hierarchical localization needs more test in different group size. For distance based localization, selection of the length scale is subjective and requires trial-and-error.

CHAPTER VI

CONCLUSION

In this thesis, we have investigated the relative performance of three ensemble based methods: Ensemble Kalman Filter (EnKF), Ensemble Smoother (ES) and Ensemble Smoother with Multiple Data Assimilation (ES-MDA), for production data history matching. EnKF, ES and ES-MDA are mathematically formulated and tested on a synthetic nine-spot case and the Goldsmith field case. The synthetic case includes matching of bottom-hole pressure, water cut and gas oil ratios and is used to validate the method. The field example consists of 31 producers and 11 injectors. The quality of the history match (water-cut, bottom-hole pressure), parameter (log permeability) estimation, variance of final updated permeability compared to the reference model permeability, etc have all been investigated to determine the performance of each approach.

Based on the results in this study, the following conclusions and recommendations are made.

1. Ensemble Smoother with Multiple Data Assimilation can be a viable alternative to EnKF. ES-MDA provides comparable production data history matching quality with better computational efficiency compared to EnKF.

2. The main advantage of ES-MDA is that it can update the reservoir model without associated stops with restarts for each ensemble member.

3. For the synthetic case and the Goldsmith field case, ES-MDA has better history matching quality and smaller root mean square (RMS) errors. The computational time is one third of EnKF for the synthetic case and about half of EnKF for the Goldsmith field case.

4. ES performed poorly compared with EnKF and ES-MDA in terms of history matching quality; however, ES has best computational efficiency among the three ensemble methods.

5. For the Goldsmith field case, four data assimilations are found to be enough to provide good production data history matching. Larger number of data assimilations consume more computation time, but lead to relatively small history matching improvement; smaller number of data assimilations is more computational efficient, but sacrifice the history matching quality. In summary, four data assimilations are a balance between history matching quality and computational efficiency.

6. The use of the inflation coefficient in a deceasing order resulted in small improvement compared with all inflation coefficients being equal to the number of data assimilations.

7. Three localization methods have similar performance. Hierarchical localization needs more test with different group sizes. For distance based localization, selection of the length scale is subjective and requires trial-and-error.

REFERENCES

A.C. Reynolds, M. Z. a. G. L. (2006). "Iterative Forms of the Ensemble Kalman Filter." *10th European Conference on the Mathematics of Oil Recovery*.

Anderson, J. L. (2003). "A Hierarchical Ensemble Filter for Data Assimilation." *Monthly Weather Review*, **131**, 634.

Anderson, J. L., and Anderson, S.L. (1999). "A Monte-Carlo Implementation of the Nonlinear Filtering Problem to Produce Ensemble Assimilations and Forecasts." *Monthly Weather Review,* **127**(12): 2741-2758.

Arroyo, E., Devegowda, D., and Datta-Gupta, A. (2006). "Streamline-Assisted Ensemble Kalman Filter for Rapid and Continuous Reservoir Model Updating." *SPE Reservoir Evaluation & Engineering,* **11**(6): 1046-1060.

Aanonsen, S. I., Nævdal,G.,Oliver,D.S.,Reynolds,A.C.,Valle´ s, B. (2009). "Review of ensemble Kalman filter in petroleum engineering." *SPE Journal* **14**(3): 393-412.

Alexandre A. Emerick, A. C. R. (2012). "History-Matching Production and Seismic Data in a Real Field Case Using the Ensemble Smoother With Multiple Data Assimilation." *SPE Journal* **11**(2): 271-287.

Alexandre A. Emerick, A. C. R. (2013). "Ensemble smoother with multiple data assimilation." *Computers & Geosciences* **55**(6): 3-15.

C.L. Keppenne, M. M. R. (2003). "Assimilation of temperature into an isopycnal ocean general circulation model using a parallel ensemble Kalman filter." *Journal of Marine Systems* **40**: 363-380.

Emerick, A. A., Reynolds,A.C (2011). "History matching a field case using the ensemble Kalman filter with covariance localization." SPE Reservoir Evaluation & Engineering **14**(4): 423-432.

Evensen, G. (1994). "Sequential data assimilation with a nonlinear quasi-geostrophic model using Monte Carlo methods to forecast error statistics." *Journal of Geophysical Research* **99**(C5): 10143-10162.

G. Evensen, P. J. v. L. (2000). "An ensemble Kalman smoother for nonlinear dynamics." *Monthly Weather Review* **128**(6): 1852-1867.

I. Szunyogh, E. J. K., G. Gyarmati, D.J. Patil, B.R. Hunt, E. Kalnay, E. Ott, J.A. Yorke (2005). "Assessing a local ensemble Kalman filter: perfect model experiments with the national centers for environmental prediction global model." *Monthly Weather Review* **57**: 528-545.

Liu, N., & Oliver, D. S (2005). "Critical Evaluation of the Ensemble Kalman Filter on History Matching of Geologic Facies." *SPE Journal* **6**(3): 344-367.

Nævdal, G., Mannseth,T.,Vefring,E.H. (2002). "Near-well reservoir monitoring through ensemble Kalmanfilter." *Proceedings of the SPE/DOE Improved Oil Recovery Symposium*.

Oliver, D. S., Chen,Y. (2010). "Recent progress on reservoir history matching: a review." *Computational Geosciences* **15**(1): 185-221.

P.J. van Leeuwen, G. E. (1996). "Data assimilation and inverse methods in terms of a probabilistic formulation." *Monthly Weather Review* **124**: 2898-2913.

Skjervheim, J., & Evensen, G (2011). "An Ensemble Smoother for Assisted History Matching." *SPE Journal* **5**(2): 412-423.

Y. Chen, D. Z. (2006). "Data assimilation for transient flow in geologic formations via ensemble Kalman filter." *Advances in Water Resources* **29**(8): 1107-1122.